Durham E-Theses

Vernier hybrid wind turbine generators

Roding, Wernher Erich

How to cite:

Roding, Wernher Erich (2001) *Vernier hybrid wind turbine generators*, Durham theses, Durham University. Available at Durham E-Theses Online: http://etheses.dur.ac.uk/3802/

Use policy

The full-text may be used and/or reproduced, and given to third parties in any format or medium, without prior permission or charge, for personal research or study, educational, or not-for-profit purposes provided that:

- a full bibliographic reference is made to the original source
- a link is made to the metadata record in Durham E-Theses
- the full-text is not changed in any way

The full-text must not be sold in any format or medium without the formal permission of the copyright holders.

Please consult the full Durham E-Theses policy for further details.

Academic Support Office, Durham University, University Office, Old Elvet, Durham DH1 3HP
e-mail: e-theses.admin@dur.ac.uk Tel: +44 0191 334 6107
http://etheses.dur.ac.uk

7465
01

Vernier Hybrid Wind Turbine Generators

Wernher Erich Roding

The copyright of this thesis rests with the author. No quotation from it should be published in any form, including Electronic and the Internet, without the author's prior written consent. All information derived from this thesis must be acknowledged appropriately.

M.Sc. Thesis

Electrical Power and Control
School of Engineering
University of Durham

2001

26 APR 2002

Abstract

A great deal of research is currently being undertaken in the field of renewable energy, much of it dedicated to wind power conversion and focussing on a machine topology that increases efficiency. The vernier hybrid machine, VHM, is one topology considered and has promising features for use in direct drive and variable speed operation.

Using the VHM topology, two prototype generators were built and tested. The machines use magnets that are buried within the stator and orientated in a flux concentration arrangement. The flux paths in the machines are inherently 3D in nature and thus require complicated modelling methods to achieve sufficient design accuracy. Various tests were conducted in an effort to find results that will describe the machines characteristics and operating mechanisms. It was found that increased torque handling capabilities can be observed at the detriment of power factor and construction complexity.

With the use of power factor correction and suitable construction techniques the VHM is a viable wind turbine generation technique. To determine whether it is suitable for renewable energy applications would require an in depth economic feasibility study over the operating lifetime of the machine.

Copyright

The copyright of this thesis rests with the author. No quotation from it should be published without their prior consent and information derived from it should be acknowledged.

Declaration

None of the work contained in this thesis has been submitted by the author for a degree at the University of Durham or any other university. The work contained is my own and is submitted without contributions from anyone else.

Acknowledgements

I have learned a great deal and thoroughly enjoyed my time at the University of Durham. The University and specifically the Engineering Department are to be congratulated for providing excellent facilities with a great atmosphere.

I would especially like to thank Professor Ed Spooner for inviting me to come and study at Durham and supervising my M.Sc. I must also acknowledge Markus Mueller, Jim Bumby and Janusz Bialek for being available with academic support and always willing to help.

Thanks to the guys in the lab, specifically Ted, who worked very hard and accurately to construct my machine. In addition, my time was made even more enjoyable thanks to Mark, Nick and Paul for their entertainment value if nothing else.

I must also thank my parents for encouraging me to come to the UK to study and for providing support throughout my entire education.

And not to be forgotten, I would like to thank my fiancé and soon to be wife Arna for packing up and coming all the way to the UK with me. I would not have come without you.

Contents

List of Figures

List of Tables

Lists of Symbols and Abbreviations

Symbol	Description	Unit	Symbol	Description	Unit
A	Area	m^2	N	Number of turns	
B_{ag}	Airgap flux density	T	P	Real power	W
B_r	Remnant flux density	T	Q	Reactive power	Vars
B_{sat}	Saturation flux density	T	r	Radius	m
C	Capacitance	F	R	Resistance	Ω
C_p	Turbine coefficient		S	Reluctance	A/Wb
E,e	emf	V	V	Voltage	V
F	Force	N	Vel	Velocity	m/s
f	Frequency	Hz	V_{l-l}	Line-line voltage	V
g	Airgap length	m	V_{l-n}	Line-neutral voltage	V
H_c	Coercive force	A/m	Vol	Volume	m^3
I	Current	A	Z	Impedance	Ω
K	Electric loading	A/m	θ	Angle	Degrees
l	Length	m	μ	Permeability	H/m
L_m	Mutual inductance	H	μ_{rec}	Recoil permeability	H/m
L_s	Synchronous Inductance	H	σ	Shear stress	N/m^2
L_{self}	Self inductance	H	τ	Torque	Nm
M_l	Magnet length	m	Φ	Flux density/magnetic loading	Wb
M_t	Magnet thickness	m	ψ	Flux linkage	Wb
M_w	Magnet width	m	ω	Angular velocity	rad/s

Abbreviation	Description	Abbreviation	Description
AFVHM	Axial flux vernier hybrid machine	PWM	Pulsed width modulation
BMVHM	Buried magnet vernier hybrid machine	SMVHM	Surface mount vernier hybrid machine
FEA	Finite element analysis	TFM	Transverse flux machine
FRM	Flux reversal machine	VAWT	Vertical axis wind turbine
HAWT	Horizontal axis wind turbine	VHM	Vernier hybrid machine
LSM	Least squares method	VRM	Variable reluctance machine
NdFeB	Neodymium Iron Boron	WEC	Wind energy converter
PM	Permanent magnet	RPM	Revolutions per minute

1.0 Introduction

Substantial research is currently being undertaken in the field of alternative energy as the demand for renewable energy sources increases. The main reason for this is that the human race now realises that unsustainable resources are limited and what is being utilised is adversely affecting our environment. But the underlying problem with extracting energy from renewable resources such as wind, tidal, solar etc., is that the power extraction is not efficient enough to justify the greater expense over existing methods. Especially for an amount of generated power that is comparatively negligible.

One avenue of research has been to try and develop a generator that does not require mechanical gearing to the prime mover as this is both less expensive and more efficient. With respect to electrical generation this method of coupling is referred to as direct drive. At The University of Durham extensive research is being conducted on vernier hybrid machine (VHM) technology for direct drive applications. The suitability of the VHM for direct drive wind power applications is derived from its high torque handling capabilities for a relatively compact size at low synchronous speeds. With the addition of power electronics the variable speed mode of operation may also be utilised and efficiency increased.

The final objective of this one-year MSc is to have tested a buried magnet VHM (BMVHM) and have designed and constructed an optimised axial flux buried magnet vernier hybrid machine (AFVHM). The aim of this work being to uncover the operating mechanisms and to test the hypotheses associated with the buried magnet topology.

The purpose of this thesis is to familiarise the reader with the work and findings developed over the past year. The basic principles of machine theory used to determine optimisation are presented. Wind turbine operation, standard formations and current ideas for efficiency improvement are studied. As a prototype was designed, the design processes are explained and their accuracy analysed.

A description of the VHM topology and its operating principles are reviewed as a leader to the analysis of the design, construction and testing of both the BMVHM and AFVHM. Comparisons to the accuracy of models and the test results is shown and the reasons for

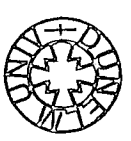

discrepancies explained. Finally the work is discussed and future recommendations are made and conclusions presented.

As the majority of design work for the BMVHM has been focused on producing an electrical generator it will be this application that will be described throughout the remainder of the thesis. Most concepts described are also attributable to the motoring mode of operation. A very promising application for this new topology is for use in alternative energy systems (mainly wind, wave and tidal power) and as a result these will be the major applications discussed. There are other applications suited to this topology that will also be examined.

1.1 VHM History

The VHM topology is a new and unique variation of a high power density machine using permanent magnets. As permanent magnet materials have improved in cost and material properties over the last few decades, much interest has been shown with respect to utilising their properties for electrical generation and motoring.

Weh et al [1] developed a permanent magnet machine that incorporates properties ideally suited for high power applications at reduced size. This machine was named the transverse flux machine (TFM) and was constructed in a rather complicated fashion, Fig. 1.1. It utilises the magnet flux concentration technique with axial linkage flux via the claw pole configuration. The claw pole nature of the design enables independent 3D flux paths but greatly complicates the design and construction processes.

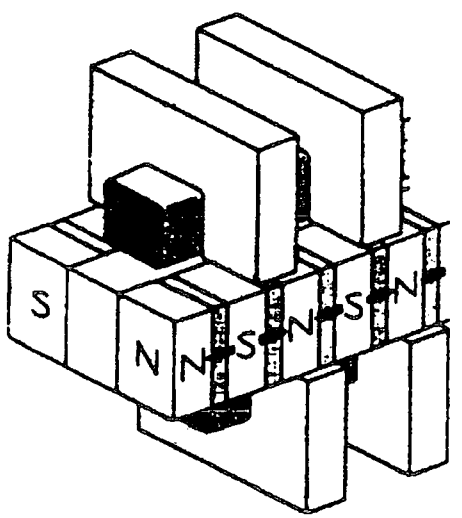

Fig. 1.1: The TFM [1]

Mecrow and Jack [2] developed a high torque vernier reluctance machine (VRM) with the same characteristics of the TFM but not reliant on the claw pole design, Fig. 1.2. The rotor holds the magnets whilst the stator modulates the radial flux so that it links discrete windings and utilises the vernier modulation method. This variation recognises the benefits of a double-sided design with flux concentration.

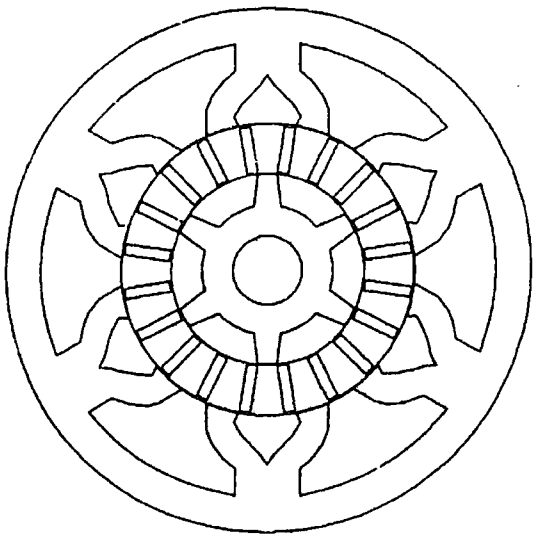

Fig. 1.2: The VRM [2]

Deodhar et al [3] created the flux reversal machine (FRM) which holds the magnets upon the stator and has radial flux linkage, Fig. 1.3. The rotor is therefore made of solidly joined laminations and is hence robust and well suited to high speed applications.

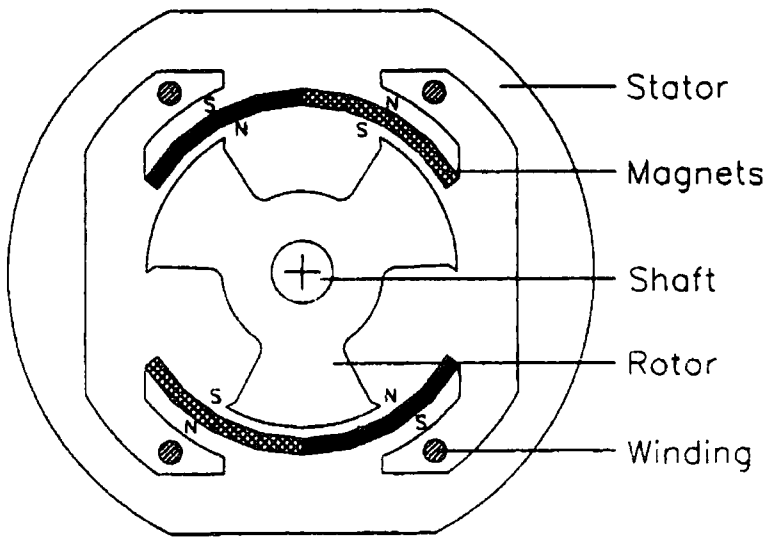

Fig. 1.3: The FRM [3]

One common relationship between all these machines is the modulation of flux by the interaction of magnets and teeth which implies use of the variable reluctance mechanism. The VHM uses this principal also but differs as the magnets are mounted upon the stator and modulate the flux in the vernier manner. Discrete coils are also mounted on the stator with the magnets. The VHM therefore contains characteristics from the TFM, VRM and the FRM. This design provides some interesting advantages as well as numerous variations with differing characteristics. It is this topology that is represented in this thesis.

2.0 Important Concepts

2.1 Shear Stress

Shear stress is a very useful concept in machine theory. It is a way to normalise the performance of different machines and is related to the level of magnetic and electric loadings within the machine. It describes the interactive forces that appear on the surface of the rotor and stator that provide the torque necessary for mechanical or electrical power generation. The higher the shear stress the higher the torque and output power capability for a given machine size and rated speed. Limitations are placed on shear stress by the material properties of the machine, these are primarily: saturation (due to magnetic loading) and thermal tolerances (due to electric loading) and the demagnetisation limitations of the magnets.

There are two primary methods of characterising typical electrical machines, those that produce torque via the interaction of currents and magnetic fields (Lorentz force) and those that operate by reluctance variation [4]. Fortunately both methods can be described by the Lorentz force, which simplifies matters and adds a method for comparison.

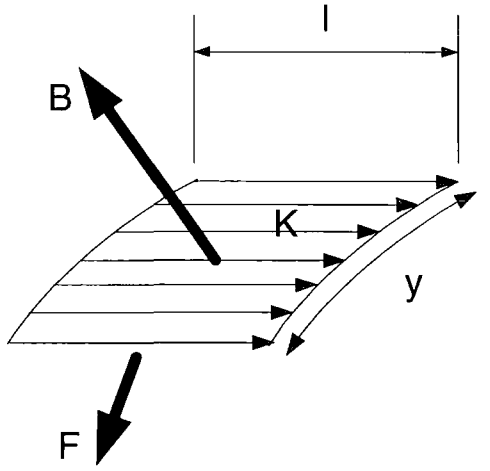

Fig. 2.1: Small rotor area displaying fields and parameters

To understand the principal of shear stress, consider a small rectangular area in the airgap and assume that this area has a radial flux density (B) perpendicular to it, Fig. 2.1 [5]. Also assume that the flux density is produced by an independent source fixed to the rotor i.e., permanent magnet. The value of flux density is defined by various machine parameters which make the magnetic circuit. Let the current that flows across this area be associated

with the stator and be defined in amperes (I). The electric loading (K) in Amps/m, is hence equal to I/y when considering arrays of conductors. The force created by the interaction of flux and current is given by the Lorentz law, Eqn. 2.1, and as the shear stress (σ) is a measure of the electrical and magnetic loadings, it can be described by Eqn. 2.2.

$$F = BIl = BKyl \qquad \text{Eqn. 2.1}$$

$$\sigma = BK \qquad \text{Eqn. 2.2.}$$

It is equally viable to model a magnet by a set of current sheets, Fig. 2.2, and therefore define the electric loading by Eqn. 2.3, where B is now related to the maximum flux density achievable in the airgap [4]. This enables the Lorentz force calculations to be used to determine shear stress for a machine using reluctance variation by simple substitution, Eqn 2.4.

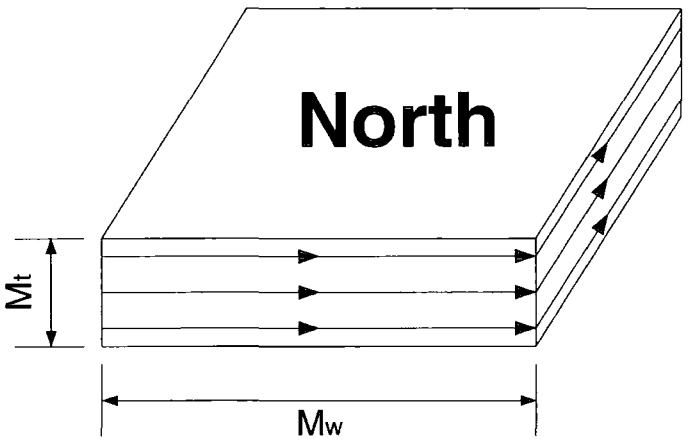

Fig. 2.2: Current sheet equivalent for a magnet

$$K = \frac{H_c M_t}{M_w} \qquad \text{Eqn. 2.3}$$

$$\sigma = B\frac{H_c M_t}{M_w} \qquad \text{Eqn. 2.4}$$

As both the electric loading and flux density distributions are likely to be sinusoidal, the mean value of shear stress is half the peak. To put mean shear stress in terms of torque, the force is simply multiplied by the rotor radius to provide Eqn. 2.5, where y is replaced by the rotor circumference. The units for shear stress are N/m^2 or more typically kN/m^2.

$$\tau = 2\sigma \underbrace{\pi r^2 l}_{rotorvolume} \qquad \text{Eqn. 2.5}$$

Eqn. 2.5, shows that the physical size of the machine is directly related to the amount of torque it can process. The torque/volume relationship is not linear as larger machines can exhibit higher torques as they are easier to cool and hence the electric loading restrictions are increased [6].

Another concept called specific torque is closely related to shear stress and is defined as torque per rotor unit volume. This is equal to the peak shear stress or twice the mean shear stress and is a measure used to compare the size of the machine to its torque capability (or power to weight ratio). Table 2.1 contains some typical values of shear stress for more common machines.

Machine Type and Size	Continuous Mean Shear Stress (kN/m^2)
Fractional TEFC industrial motors	0.7-2
Integral TEFC industrial motors	7-15
High performance industrial servos	10-25
Aerospace Machines	25-35
Very Large Liquid Cooled Machines	60-110

Table 2.1: Various shear stress values for common motors [5]

2.2 Direct Drive

The concept of direct drive refers to an electrical machine that is coupled to the mechanical part of a system without the use of a gearing mechanism. For most systems involving the connection of a machine to a mechanical source some form of speed or torque control is required. This is usually achieved by the incorporation of a gearbox.

In typical electrical generation terms the purpose of a gearbox is to step up or down the speed that a machine will run at, so that the generators rated speed effectively matches that of the prime mover. By doing this common synchronous and inductance machines of convenient size can be used. To be able to omit the gear box would either mean that the system being fed does not require any frequency or voltage matching, the machine is driven at a constant speed that matches the frequency of the system or it has power electronics incorporated.

There are certain disadvantages involved with the use of a gearbox. Firstly they are a source of mechanical power loss. This is significant when applications for alternative energy are considered as efficiency is of key importance. Secondly as a gearbox is a mechanical component there is the need for continual maintenance. If the machine is situated in a remote location, for example in a wind farm placed offshore, maintenance becomes expensive and arduous. As the gearbox is another component it will also add to the overall system cost.

2.3 Variable Speed

For some applications controlling the speed of the prime mover can be inefficient. For these types of applications it would be desirable to have a generator that would produce maximum power over a range of speeds. A design like this would work well with a direct drive system. Unfortunately most loads require an electrical input that has stable frequency and magnitude.

To match the frequency of the source to that of the load without mechanical means would require electronic control. This control would use power electronic inverters which can provide desired frequencies at required voltage magnitudes. At present, electronics are becoming more sophisticated at more reasonable prices, which is making the use of power electronics more viable.

2.4 Magnetic Materials

2.4.1 Permanent Magnets

Permanent magnets (PM) are made from hard magnetic materials that retain significant magnetisation with the retraction of an applied magnetic field. With the development of better PM materials such as, neodymium iron boron (NdFeB) the number of applications they are suited for have increased. As the price for PM materials continues to decrease, their use in machine production becomes more feasible. This has led to a lot of research into the use of PM's.

A PM material can be characterised by the relationship between flux density (B) and applied magnetic field strength (H). This relationship is plotted in a B-H curve, Fig. 2.3. From the B-H curve the important characteristics of the magnet can be determined. These are: remnant flux density (B_r) and coercive force (H_c).

To obtain the B-H curve an unmagnetised piece of magnetic material is subjected to an increasing mmf. The applied field is increased until the flux density of the magnetic material increases no further (saturation flux density). The field is then reduced until no field remains, the value of flux density retained within the material at this point is the remnant flux density. The direction of the applied field is now reversed until a negative value of saturation flux density is achieved. The intercept with the horizontal axis is the applied field needed to depolarise the magnet and is known as the coercive force. The applied field is now increased until positive saturation flux density to complete the loop.

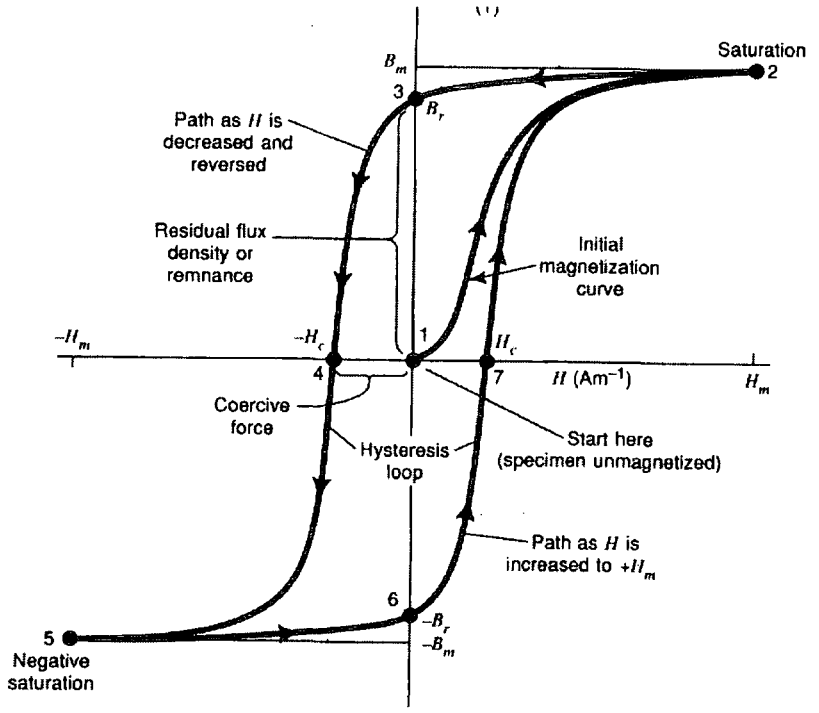

Fig. 2.3: Typical BH curve [7]

The material properties of a PM alter when subjected to various conditions. When a magnet is exposed to higher temperatures, the material properties begin to change and the magnetisation decreases, the rates of which depend on duration and temperature. Above a certain temperature known as the Curie temperature, a magnet will become fully depolarised. If no metallurgical changes have taken place it is possible to re-magnetise the magnet.

2.4.2 NdFeB

NdFeB magnets have very impressive qualities compared to other magnetic materials, Fig. 2.4. They typically have a B_r=1.2T and H_c=900kA/m. The characteristic of NdFeB in the

second quadrant of the BH curve is nearly linear with a low gradient which implies that the magnet can operate at high flux densities in the presence of an applied field.

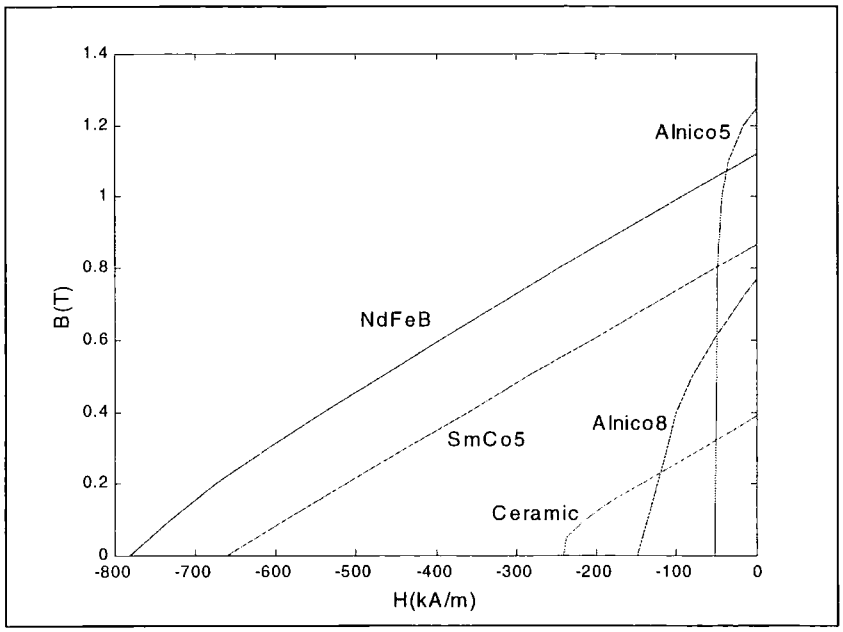

Fig. 2.4: Magnet material BH curve comparison

NdFeB has a good recoil permeability which means that once an applied field has been removed, the magnet will return to the point on the BH curve before the field was applied. This is only the case for operation in the second quadrant. This quality makes NdFeB easier to analyse and ensures a constant operating range when in use. Appendix A shows some of the important properties of the N30 NdFeB material used for the prototypes.

2.4.3 Saturation

Saturation is one of the major factors to be considered for any application using magnetic fields. Saturation is the point where all of the magnetic dipoles in a magnetic material have been polarised. This adds nonlinearity into any calculations where the material may operate up to the saturation region. Once saturation is reached, the magnetic loading can no longer be increased and the machine runs at a lower efficiency for any further electric loading increases. Therefore machines are designed so that they do not fall into heavy saturation within their operating limits.

3.0 Wind Power

3.1 Wind Energy Converters

The use of wind energy converters (WEC) is one of the more promising alternative energy topologies available for use in the near future. The problem associated with a WEC is the vast area needed to produce the equivalent power to that of a hydro, coal or nuclear power station. With current WEC sizes of 1.5-3MW per unit, at least 300 units would be needed to generate the equivalent of a 1GW station. With this in mind, the efficiency of the overall turbine system must be maximised so that peak power is extracted for a given size and cost.

The amount of power that can be extracted from the wind over a fixed area is limited and defined by the Betz Limit, which states that no more than 59.3% of the power in an area of wind can be utilised. The mechanical power that can be generated from the wind can be obtained from Eqn. 3.1, and is related to air density (ρ), the velocity of wind (Vel) and a factor that relates to the turbine specifics (C_p). C_p is a function of blade aerodynamics, wind angle to the turbine, etc. Next the electrical generator must convert the mechanical input power to electrical. Fig. 3.1, shows a typical wind turbine system.

$$Pwind = \frac{1}{2}\rho A Vel^3 0.593 C_p \qquad \text{Eqn. 3.1}$$

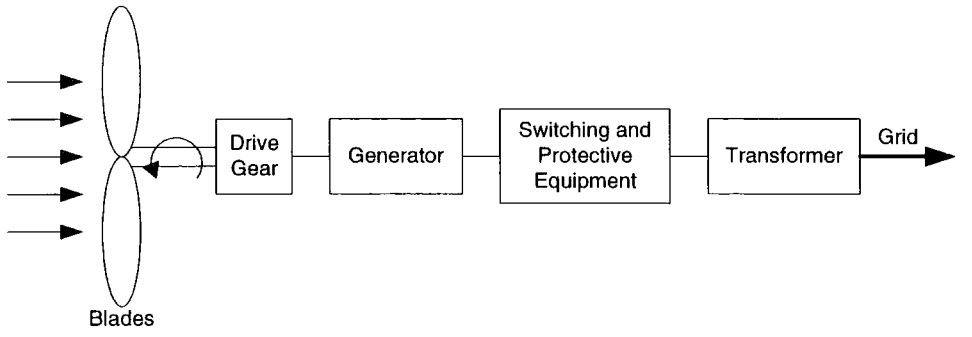

Fig. 3.1: Typical wind turbine system

Wind turbines come in many different forms but can be separated into two main categories: horizontal axis wind turbine (HAWT) and vertical axis wind turbine (VAWT), Fig. 3.2. The most common of these two by far is the HAWT. The HAWT does have two disadvantages over the VAWT. As the axis is horizontal, it is most efficient to have the

electrical generator situated at the top of the tower as to avoid any complicated and inefficient coupling. The tower must be well designed and constructed of strong materials as it must be able to support the combined weight of the turbine and generation system with the added force applied by the wind. This makes the tower and nacelle a significant cost component in HAWT design.

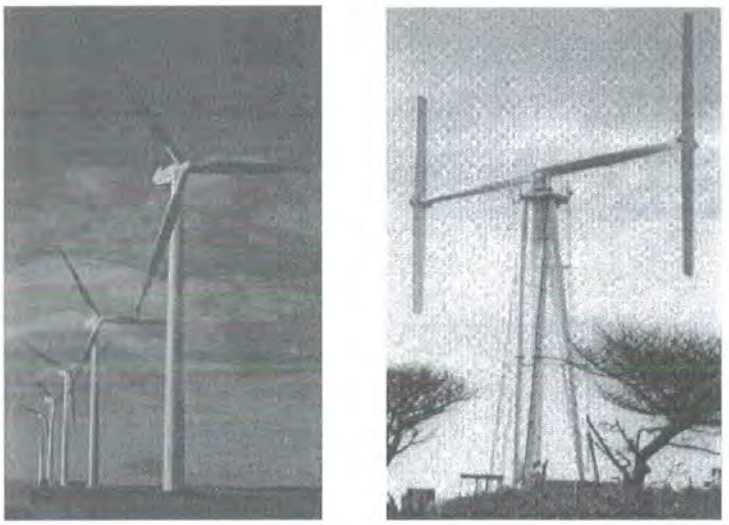

(a) (b)

Fig. 3.2: Typical HAWT (a) [7] and VAWT (b) [8]

The VAWT can easily be directly coupled via a shaft to a generator situated at ground level, this would negate any need for a strong tower. The VAWT can also rotate at maximum efficiency with an incident wind angle of any value, but an external force must be applied to start rotation. This could be done with a small induction motor. As a HAWT is susceptible to the wind angle, a method of direction control must be incorporated so that the HAWT is operating at optimum efficiency to the prevailing wind. This involves control systems, servomotors and transducers, all of which add weight, cost and additional power consumption.

3.2 Wind Turbine Improvement

As peak efficiency and economic viability are desired, components that provide losses and cost must be analysed and their necessity considered. One such component is the gearbox. This component comes with all the undesired characteristics as explained previously. With respect to wind turbines however, there are other factors that gearboxes introduce that need to be considered.

As a gearbox is mechanical, the moving parts create a certain amount of undesirable noise [8]. If a large wind farm is established this noise can become quite substantial and an annoyance to residents within the vicinity. As a result planning consent to construct a wind farm may then become difficult to obtain. Another important consideration for wind turbine construction is the weight of the turbine (including all the generating components) as this will greatly affect the design of the tower. Obviously a lighter turbine is desired so that tower cost can be minimised, omission of a gearbox would definitely result in a weight reduction.

Until recently the gearbox has been an essential component in wind turbines due to the use of synchronous and induction generators at a convenient size. A wind turbine rotates at low speed but synchronous and induction generators of conventional pole number need to rotate considerably faster to achieve the output frequency of 50Hz and rated voltage to match the grid. This is why a gearbox, that steps up the rotational speed is used. A direct drive system powers the generator directly from the prime mover and hence renders the gearbox obsolete.

Synchronous and induction generators can be used for direct drive applications but are usually designed with a much larger diameter to accommodate the increased pole number and to increase the tip speed of the rotor for a constant speed of rotation.

Wind speed is variable, thus power is only generated over a certain range of speeds and is related to the rated values of the generator and mechanical tolerances of the turbine. Fig. 3.3, shows a typical power curve for a conventional WEC system. To keep the generator within its rated region blade pitch control or electrical braking are used. Blade pitch control alters the incident angle of the blades to the wind so that the turbine produces less or more power. By reducing the power, there is obviously potential energy being lost. It would be desirable to be able to produce power over a larger wind velocity range and hence utilise all the energy available. This would require a variable speed machine. It is estimated that 10-15% more power can be extracted from variable speed generation in wind turbines [9]. One limitation that is unavoidable is when the wind velocity is too high and the wind turbines mechanical tolerances are met, the turbine shuts itself down and does not produce power.

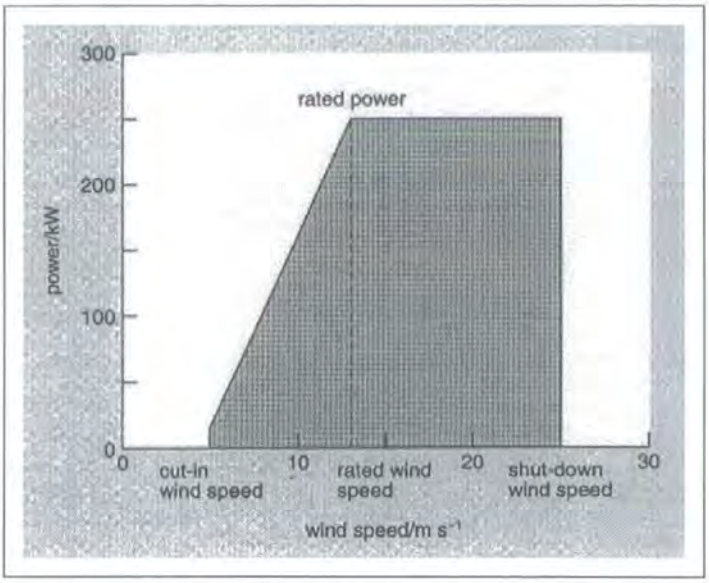

Fig. 3.3: Wind power generation curve [8]

An advantage of variable speed generation is the reduced peak torque on the blades [10]. As the blades rotate at whatever the wind speed dictates, energy from gusts can be transferred to the blades as rotational energy and converted when the gust dies. This form of damping results in less fatigue on the turbines mechanical parts which results in decreased maintenance requirements, less robust structural design and a longer operational life time.

3.2.1 Power Electronics

A typical WEC that uses induction or synchronous generators has reactive power compensation and grid synchronisation electronics. A variable speed generator also needs power electronics so that the variable nature of the output can be converted to match the system. These power electronics should: control frequency, control voltage magnitude, control reactive power, minimise harmonics and operate at a good efficiency. The most likely system to be incorporated is the AC-DC-AC system, where the variable output of the generator is rectified and then inverted so that it matches the load parameters.

Unfortunately power electronics are another source of cost which must be justified by any possible benefits.

4.0 Machine Modelling

When studying a new machine one of the primary objectives is to devise a model. This model should be able to accurately predict the machine characteristics for changes with any variable. By doing this a machine can be designed more efficiently and accurately. For the purposes of analysing the VHM, two primary methods of modelling were used, lumped parameter and finite element analysis (FEA). Two other methods were also studied but not used directly for the prototype designs. They are: the least squares polynomial fitting method and the magnetic load line method.

4.1 Lumped Parameter

Lumped parameter analysis is used when electrical circuit principles are applied to magnetic circuits. This is possible as magnetic quantities have electrical analogues. These analogues are listed in Table 4.1 and derivations are included in Appendix B. Using these analogies, an equivalent electrical circuit can be designed that models the magnetic circuit. At this point simple circuit calculations can be performed to calculate required values.

Electrical Property	Magnetic Analogue
E, emf (V)	F_m, mmf (At)
I, Current (A)	Φ, Flux (Wb)
R, Resistance (Ω)	S, Reluctance (A/Wb)
J, Current density (A/m)	B, Flux Density (T)
σ, Conductivity	μ, Permeability (H/m)

Table 4.1: Electrical properties and their magnetic analogues

The resulting model is not comprehensive as it does not account for the non-linear affect of iron in magnetic circuits and should thus only be used as guide. Other more complex issues are also not accounted for, such as: fringing fields and iron losses. Despite its inaccuracy, lumped parameter modelling is still very useful as it provides a method that can compute with great speed. The values calculated can then be used as a starting point within FEA optimisation computations. It is not uncommon for values calculated in FEA to be transferred back into a lumped parameter system to improve accuracy and thus allow the designer to calculate with greater speed.

One difficulty associated with lumped parameter analysis is including estimations for leakage flux. Leakage flux is deemed as any flux that does not link the coils, this may be in the form of end leakage or simply flux that finds another path to complete the circuit. It

is beneficial to include these losses as they can be significant. These quantities cannot be readily defined by the simple electrical analogues and must be calculated separately. They can then be incorporated into the equivalent circuit at a later stage.

4.2 Finite Element Analysis

With the phenomenal increase in computer processing speed in recent years, finite element analysis has become commonplace. This method takes the non-linear iron and leakage effects into account and is thus more accurate. Despite faster processors, simulation times can still be long, thus making optimisation tedious.

FEA gives solutions to partial differential or integral equations that cannot be solved by analytic methods. In the case of electric and magnetic circuits Maxwell's equations are generally solved. Whilst inputting the model, the user defines a set of nodes along each boundary surface. The software then creates internal nodes that are joined together forming elements, all of the elements combined create what is called the mesh. For each element the software solves the equations that are applicable to the simulation and repeatedly does so until a specified convergence is reached. For this process to work, suitable boundary conditions must be introduced as this provides a reference point for the solutions.

Before FEA analysis can be undertaken the model must be entered into the software. A simpler model results in less processing time for each simulation. It is therefore worthwhile studying the model and determining whether the entire machine needs to be entered or perhaps just a repetitive segment. The latter is obviously preferable. Due to the low operating pole number of the VHM topologies studied there is not much advantage in simplifying the model.

After simulation, various results can be extracted depending on the software's capabilities. The programmer must also be aware that nodal positioning is important and in areas of constructional complexity and high flux density gradient the nodes should be closely spaced. Most FEA software limits the number of nodes that can be placed as they can only calculate for models with restricted complexity, the programmer must then carefully determine the nodal position.

The Vector Fields FEA software used at Durham University has many features. Those features primarily used are: flux density calculations and plots, torque calculations and potential calculations. In this case, to determine the amount of flux linkage, the potential difference in Wb/m between one side of a coil to the other is determined, then multiplied by the axial length of the machine. Other values are simply retrieved through the software.

4.3 Polynomial Fitting

By using lumped parameter and FEA together a design can be finalised more quickly than with FEA alone. But as lumped parameter does not give accurate results, the FEA fine tuning can be tedious and time consuming. It would be preferential to have a method that predicts with greater accuracy so that not so much dependency lies with FEA. The solution may be to use FEA to determine a general algorithm that can be applied to calculate the machine parameters in a computationally undemanding manner. Using the method of least squares regression and FEA this can be achieved.

The general procedure for this application involves:

- Create a FEA model for the specific topology that can alter any variable for each automatic simulation. The variable values can be obtained automatically from a file prepared earlier, most modern industrial FEA programs will provide this facility. The program can then be left to run until all the solutions are found.

- Store both the data obtained from these simulations and the variable values corresponding to each solution. Use this data to determine a general algorithm that describes the machine, in this case by using the method of least squares regression.

- Use the algorithm to optimise machine parameters with genetic algorithms and un-intensive computerised techniques.

- FEA can then be used to 'fine tune' the final design.

This process will be more efficient than using FEA exclusively as the total computation time is reduced.

The least squares method (LSM) fits a desired function to a set of input data by calculating the square of the error between the data and the result of the function that is being fitted [11]. When this error is a minimum the fitted function is close to that which defines the

input data. An important step is to determine what kind of function will fit the data, this can be done with little knowledge of the system. In most cases a polynomial will suffice.

As the order of the polynomial and number of variables increase, the complexity and calculation time of the LSM increases also, Table 4.2. It is therefore preferable to try and model the system using a low order polynomial with a small number of variables.

Function Type	Variable Number					
	1	2	3	4	5	6
Linear	2	3	4	5	6	7
Quadratic	3	6	10	15	21	28
Cubic	4	10	20	35	56	84
Fourth Order	5	15	35	70	126	210
Fifth Order	6	21	56	126	252	462
Sixth Order	7	28	84	210	462	924

Table 4.2: Number of terms for various polynomial orders [11]

In the case of the VHM an important value is the flux distribution, from this the peak flux linkage can be determined and used to calculate many parameters and performance characteristics. If the machine is to be connected to a 3 phase system the desired flux distribution is sinusoidal. To fit a polynomial to a sinusoidal signal, 3rd order or higher is needed. As a sinusoid has symmetry about half a period it would be satisfactory to model for only this displacement [12]. It is now possible to fit a 2nd order (quadratic) polynomial to the data, as long as the data is only over a displacement of a magnet pole pitch from the point of minimum linkage.

A typical VHM has many variables that need determining e.g., tooth width, magnet width, airgap length, etc. It is beneficial to reduce the number of variables if possible. Some variables may be determined by practical limits or specifications, while some might be explicitly defined by a combination of other variables effectively making them functions of that variable e.g., tooth width, slot width and pole pitch. The range of values of a variable will also determine system accuracy and computation time. A variable's range can be decreased by considering: practical limits, specifications and common sense.

It is also beneficial to simplify the model that is simulated in the FEA as the larger the model the longer the simulation time. Model simplification can be achieved by identifying a repeated unit in the machine topology and only modelling for this unit. When the results are found simply multiply them by the number of units.

The data used to obtain the polynomial must fully encompass the design space else the result will not satisfactorily match the system. Two methods can be used to determine the source data points. One is a random method which relies upon statistics to place data points adequately in the design space. This method is subject to "bad luck" and with a small number of points may not cover the design space. The other method is a manual grid that encompasses points evenly throughout the design space. This results in a large number of data points depending on the resolution determined for each variable. Fig. 4.1 shows a comparison of random and manual grid data selection for the VHM, in this case the error associated at peak flux linkage is approximately equal for each case.

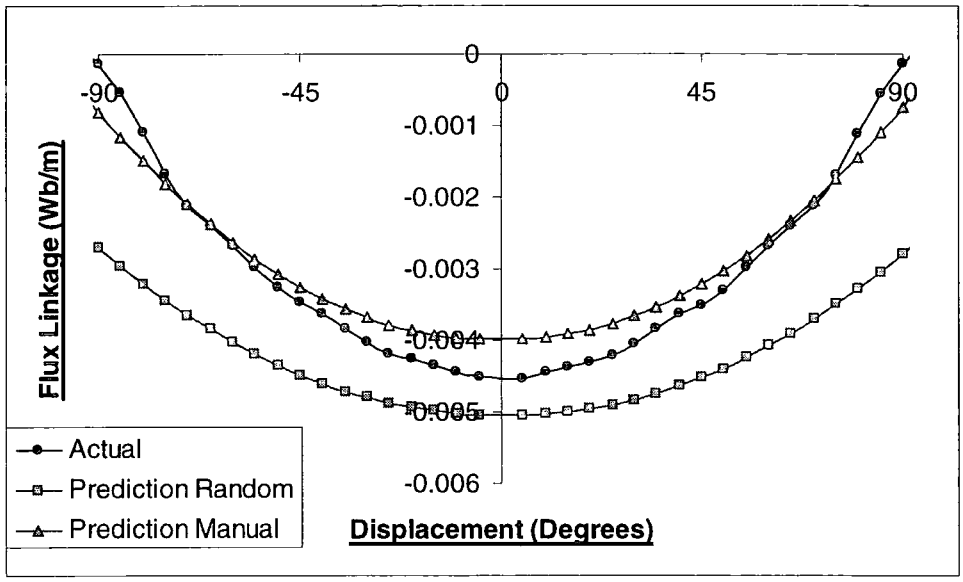

Fig. 4.1: A comparison of FEA and the LSM for the VHM

4.4 Magnetic Load Line

Unlike lumped parameter analysis, the magnetic load line method can account for non-linearity but should still only be used as a design guideline. To incorporate non-linearity this method uses the hysteresis curves for both the magnet and steel material. The load line method is faster than lumped parameter but can be more inaccurate as it is difficult to incorporate leakage into the calculations.

For the magnetic load line design conducted, only the magnet B-H curve is used thus ignoring the non-linearity of the iron. By defining the length of the airgap (l_a) in the magnetic circuit whilst making the assumption that steel has infinite permeability, a simple relationship between the flux density in the airgap (B_{ag}) and magnetic field strength of the magnet (H_m) is found, Eqn. 4.1. This relationship when plotted for the second quadrant of

the BH curve forms a straight line through the origin with a slope proportional to the magnet thickness and airgap length. This line is called a load line and the point at which it intersects the B-H curve of the magnet being used defines the operating flux density and hence flux from the magnet.

$$B_{ag} = -\mu_0 \frac{M_t}{l_a} H_m \qquad \text{Eqn. 4.1}$$

The second quadrant for NbFeB magnets exhibits a straight-line characteristic. It is therefore possible to simultaneously combine Eqn. 4.1 and that for the magnet, Eqn. 4.2, into one equation [7].

$$B = \frac{B_r}{H_c} H + B_r \approx y = mx + c \qquad \text{Eqn. 4.2}$$

$$B_{op} = \frac{\mu_0 M_t B_r H_c}{l_a B_r + \mu_0 M_t H_c} \qquad \text{Eqn. 4.3}$$

The use of this analysis could only be utilised for simple magnetic circuits. Fortunately the complex VHM magnetic circuits can be broken into repeatable units, which can be solved individually.

4.5 Series Equivalent Circuit

An equivalent electrical circuit can also be used to model an electrical machine, Fig. 4.2. This circuit models the machine as it is "seen" from its terminals by using a series combination of resistance and inductance. The resistance is basically the resistance of the coils R_c and the inductance is the sum of self and leakage synchronous inductances of the machine, L_s. The mutual inductance, L_m, between phases can be represented as additional series inductance in each phase. These values are only viable if the machine is balanced and feeds a balanced load, if not then full circuit representation is needed. This circuit can only be used correctly after an accurate design procedure or measurement has been used to determine the variables. By inserting a load impedance, Z_l, the machine can be modelled under operating conditions.

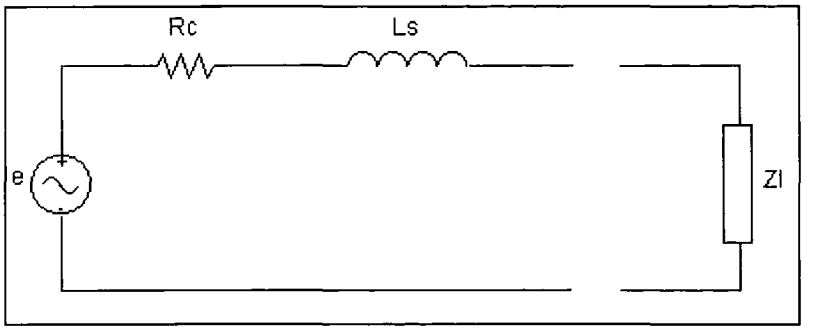

Fig. 4.2: Synchronous series equivalent circuit

5.0 Vernier Hybrid Machines

The Vernier Hybrid Machine (VHM) is an electrical machine topology that incorporates facets of the variable reluctance machine, flux reversal machine and transverse flux machine, hence the use of the term hybrid in the title. The term vernier originates from the likeness of the way the magnet poles and rotor teeth align to that of the vernier gauge and is present when the number of magnet poles to rotor teeth differs [5].

5.1 Terminology

As the VHM is largely an unrecognised topology it is appropriate to explain some of the terminology that will be used to describe specific machine components. This is done with reference to the particular configuration illustrated in Fig. 5.1. The VHM uses a large number of permanent magnets in conjunction with a large number of teeth, which complicates the terminology if trying to use conventional machine terms. To assist with clarity, for the remainder of the thesis it will be assumed that the magnets are mounted on the stator and the teeth located on the rotor, which is the VHM topology.

- Each magnet presents one magnetic pole to the airgap field. The field produced by a magnet will be referred to as a "magnet pole".

- The flux distribution determines the pole number of the machine as a whole. To distinguish this from any references to magnet poles it will be referred to as "2-pole", "4-pole" flux distribution etc.

- Pole pitch will be used in its normal manner as the rotor displacement needed for flux flow to change polarity.

- Currently the VHM has been built with very simple concentric windings, each coil being wound about a large tooth on the stator. These teeth will be referred to as the "stator poles".

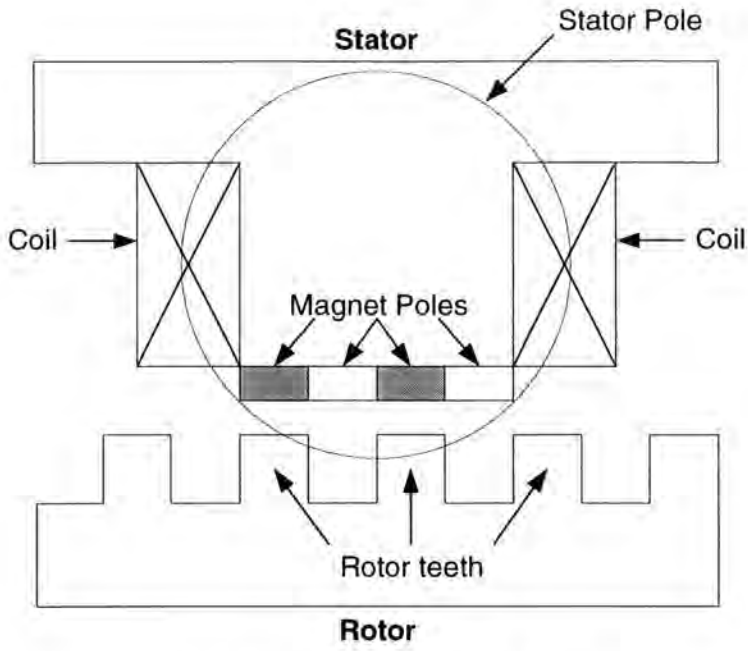

Fig. 5.1: Components of the VHM

5.2 VHM Principles of Operation

A typical three phase synchronous machine will have pole numbers of two or four, and will need to rotate at 3000RPM or 1500RPM respectively to produce an output frequency of 50Hz and rated voltage. The VHM however can produce a 50Hz output and significant voltage while rotating at much slower speeds with comparable pole flux distributions. The torque handling capability of the VHM is also increased through magnetic gearing and the use of permanent magnets.

5.2.1 Airgap Reluctance Variation

The main mechanism of the VHM is the ability to reverse the flux polarity for a small value of rotor displacement. This is achieved by the interaction of teeth, slots and magnets. As a tooth is directly inline with a magnet pole, the reluctance in the magnetic circuit is minimum and the flux linkage is a maximum. When the rotor moves a magnet pole pitch and the tooth lies directly inline with a magnet of opposite polarity the flux linkage is once again at a maximum but with direction reversed. The first magnet is now inline with a slot that provides a high reluctance to the magnetic circuit and hence very little flux flows. Therefore, the magnitude and waveform shape of flux linkage and hence emf is governed by the airgap reluctance variation.

The other topologies similar to the VHM are basically variations of magnet placement, plane of flux linkage etc. The airgap reluctance is not affected by the location of magnets and teeth as it is closely related to the length of the airgap in the magnetic circuit which is independent of magnet or tooth placement. Thus other comparable topologies can all be described in a similar manner.

5.2.2 Magnetic Gearing

Traditionally a machine with multiple poles has a larger diameter. But in a defined space a permanent magnet can provide higher flux densities to that of an excited coil with the added benefit of no excitation losses. Therefore, by using magnets instead of coils more fields of equivalent strength can be incorporated into a defined diameter or conversely the diameter can be decreased.

As the machine contains a large number of teeth and magnets compared to stator poles, the rotor displacement needed to change the direction of flux flow through a phase is comparatively small. So for one rotor revolution the flux flow changes direction more times than a conventional machine and hence the rate of change of flux is increased. This phenomenon is called magnetic gearing. Therefore by using Faradays law, for a value of low angular speed but high $d\Phi/dt$ and high flux magnitude (due to permanent magnet excitation) a considerable emf can be produced. Thus the VHM can generate higher voltages and frequencies at lower speeds than conventional machines. This has very interesting implications for direct drive wind turbine applications.

In terms of speed the magnetic gearing ratio can simply be defined as the ratio of speed of a typical machine to that of a magnetically geared machine for an equivalent generated electrical frequency and operating pole number. For example, a 2 pole (1 pole pair) synchronous machine needs to rotate at 3000RPM to produce a frequency of 50Hz, but a VHM with a 2 pole flux distribution and 20 teeth (20 pole pairs) will only need to rotate at 150RPM for the same result, Eqn. 5.1. Therefore with respect to speed in this instance, the VHM has a magnetic gearing ratio of 20.

$$f = PolePairs * \frac{RPM}{60} \qquad \text{Eqn. 5.1}$$

The magnetic gearing ratio also has a definition that pertains to torque. This relationship is more complex and difficult to accurately define as torque is a function of many variables.

It is primarily related to the number of magnet poles to one stator pole and more specifically to the number of magnet poles that conduct flux [2]. As not all of the magnet poles conduct at one time due to the topology of the VHM the magnetic loading is comparatively reduced. As the topology of the VHM is different the gearing ratio must also be adapted to account for: leakage, saliency, differing electric loadings etc.

An illuminating method of proving the higher torque capabilities of the VHM through the magnetic gearing ratio is by assuming that all the input power is equal to the output [2].

$$P = VI = \tau\omega \qquad \text{Eqn. 5.2}$$

The terminal voltage can then be determined from Faradays law.

$$V = N\frac{d\phi}{dt} = \omega N\frac{d\phi}{d\theta} \qquad \text{Eqn. 5.3}$$

And by substitution of Eqn. 5.3 into Eqn. 5.2 and solving for torque:

$$\tau = \frac{VI}{\omega} = NI\frac{d\phi}{d\theta} \qquad \text{Eqn. 5.4}$$

For a fixed magnetic and electric loading, a higher torque is produced with an increase in the rate of change of flux with respect to position. Due to magnetic gearing the VHM exhibits this characteristic and thus has high torque handling capabilities. The increase of torque from magnetic gearing is more significant than the effect of the negative factors associated with the topology e.g., not utilising every magnet pole at each moment in time.

To be able to achieve a large number of poles within a fixed machine size and maintain strong magnetic loading, permanent magnets with high B_r and H_c are necessary. There are limitations that need to be considered that affect the maximum number of poles. Increasing the number of magnets and hence frequency results in larger magnet leakage, conductor eddy current loss and iron losses. Decreasing the number of magnets for the same operating values requires larger magnets and ferrous parts and results in a larger machine [13]. The topology used ultimately depends on the application. Magnet material and dimension selection is important as the magnets provide the most significant material cost.

5.2.3 Shear Stress

A magnet occupies less space than a coil of the same mmf even if it has a very high current density. This feature is exploited in the VHM to produce high shear stress at the airgap. This is ideal for applications that have high power/torque characteristics at low speeds as the machine can be made comparatively smaller.

A hypothetical value for shear stress can be calculated by using the formulas introduced in Section 2.1 and some typical values for steel saturation of say B=1.5T and magnet properties of H_c=800kAm, M_t=6mm and M_w=30mm. The electric loading equates to 160kA/m and from the formula for shear stress, ideally values of approximately 240kN/m^2 can be achieved compared to 80kN/m^2 for a large induction machine [4].

There are limitations to shear stress as mentioned before. A major consideration is that of saturation. To achieve significant shear stress it is desirable to operate at elevated values of flux density, unfortunately the iron saturates and results in high levels of iron loss as well as inefficient machine use. Shear stress is also limited by the total current that can flow in the winding which is governed by the maximum permissible temperature of the machine.

5.2.4 Pole Flux Distribution

The vernier method of tooth and magnet pole alignment creates an unusual flux pattern within the machine core. Despite there being a large number of teeth and magnet poles the actual flux distribution will have a low pole number and as a result be similar to a typical synchronous machine, Fig. 5.2. The difference being that the VHM field rotates at a greater angular velocity.

Altering the distribution of magnet polarity can vary the pole flux distribution, Fig. 5.2. This will not have any bearing on the output frequency and voltage of the machine as it is ultimately the displacement needed for one pole pitch that defines these values for a constant speed, excitation and number of turns. Altering the flux pole number may adversely affect the iron loss as a lower pole number results in longer flux paths. Pole number can also be changed by altering the ratio of the number of teeth on the rotor to the number of magnet poles. Therefore in a VHM, it is the number of teeth and magnet alignment that determines the pole number and not the number of poles in the flux distribution. It is difficult to visualise the flux distribution within a VHM and FEA provides a convenient means of verification.

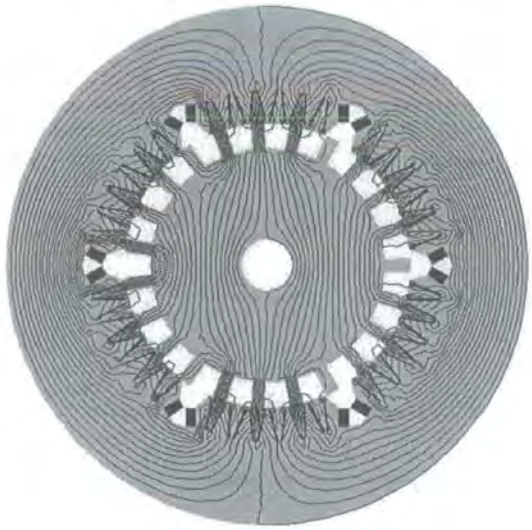

(a)

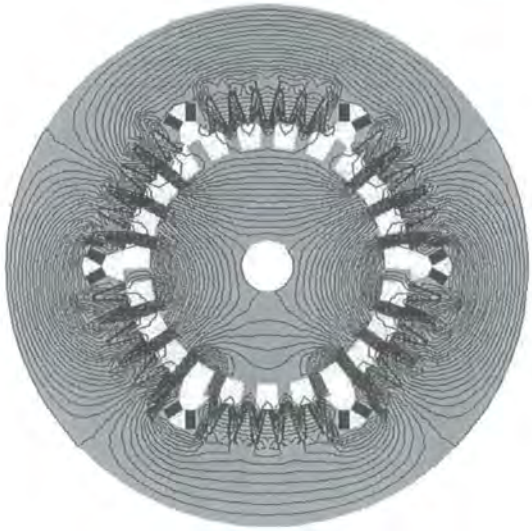

(b)

Fig. 5.2: VHM 2 (a) and 4 (b) pole flux distributions by varying magnet polarity

The vernier action conducts flux through one stator pole with a return path for the flux via a combination of other stator poles through the mechanism of rotor tooth to magnet pole overlap. In a three phase system the tooth alignment will be such so that at the instant of peak flux linkage for one phase (maximum overlap) will result in a net flux flow that has opposite polarity and half the magnitude for each of the other phases. The rotor movement will then act to increase the flux linkage in one phase (increase tooth and pole overlap), while decreasing it in the others. At the instant of zero flux linkage for a phase, the rotor tooth equally overlaps poles of opposite polarity and hence "shorts" the flux path, Fig. 5.3.

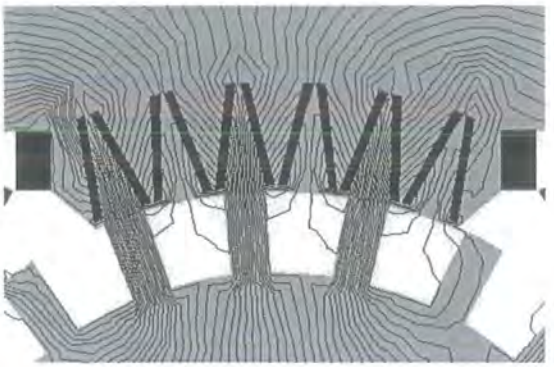

(a)

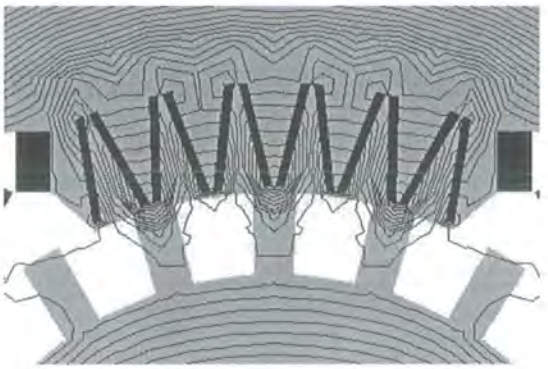

(b)

Fig. 5.3: Flux plots of maximum (a) and minimum (b) linkage for one phase

5.2.5 Low speed Operation

For applications with low speed prime movers, the VHM is a well suited generator. The mechanical power of any rotary machine is described by Eqn. 5.5. For a generator to operate efficiently at low speeds high torque handling capabilities are necessary. Shear stress is directly related to torque by the volume of the machine rotor, Eqn. 5.6. As the VHM has high shear stress characteristics, the volume/size of the machine to handle equivalent torques can be smaller. Smaller machines are advantageous as they are generally lighter and logistics can be simplified. With reference to wind power applications small generators are beneficial as the nacelle can be made smaller and the tower less rigid and hence less expensive.

$$P = \tau\omega = 2\sigma\omega * Vol_{rotor} \qquad \text{Eqn. 5.5}$$

$$\tau = 2\sigma \underbrace{\pi r^2 l}_{rotorvolume} \propto \sigma * Vol_{rotor} \qquad \text{Eqn. 5.6}$$

5.2.6 High speed Operation

By placing the magnets upon the stator of the machine the rotor can now be constructed entirely of steel laminations. As the rotor is effectively solid, it has become mechanically robust and easy to balance. This implies that the rotor could be rotated at extremely high speeds without the concern of mechanical failure. For example, if the magnets were situated on the rotor periphery the centripetal force exerted on these magnets will react with the relationship of Eqn. 5.7. Where m is the mass of the magnet, Vel is the velocity and r is the radius from the centre of rotation. Each magnet would then need a much larger force to maintain its velocity in a circular motion. The method of attaching the magnets would then require a very strong adhesive or circumferential retaining sleeve which would occupy space in the active region and thus detract from the torque

$$F = \frac{mVel^2}{r} \qquad \text{Eqn. 5.7}$$

Very high speed generation does have advantages. As the speed of rotation increases, the torque handling capability of the machine can decrease for an equivalent amount of power, Eqn. 5.5, so the volume of the rotor (and hence machine) can decrease if shear stress remains a constant. Therefore very high speed generators can be made smaller for an equivalent power demand.

One consideration at high speed is that of windage loss. Windage is the loss due to the friction of a rotating rotor with the air. At higher speeds windage increases. The VHM also has a salient rotor structure which enhances the windage factor. Windage also implies that air will circulate in the machine, if adequate ventilation is available some of the negative effects of windage balance with the supplementary cooling it provides.

Another consideration at high speed is the increased iron losses and parasitic eddy current losses due to the larger output frequency.

5.2.7 Iron Losses

Iron losses are primarily comprised of hysteresis and eddy current losses. The unutilised power (in W/m^3) from hysteresis and eddy current losses is generally defined by Eqn. 5.8 and Eqn. 5.9 [14]. It is obvious that the losses are primarily related to frequency and the maximum flux density.

To obtain high levels of shear stress the VHM must operate at high flux densities, the high pole number also leads to high frequencies. Thus the VHM is very susceptible to iron losses and must be designed accordingly.

$$P_{eddy} = \frac{\pi^2 B_{\max}^2 f^2 t^2}{6\rho} \qquad \text{Eqn. 5.8}$$

$$P_{hys} = \lambda B_{\max}^{1.7} f \qquad \text{Eqn. 5.9}$$

The primary method of minimising iron losses is to use a laminated material with high permeability and saturation flux density in the segments of the machine that carry high flux density i.e., the rotor teeth. Laminations serve to decrease eddy current losses by simply minimising the area that the induced currents caused by flux can flow, i.e., decrease t in Eqn. 5.8. The choice of magnetic material is important as both iron loss components are functions of material properties λ and ρ. By appropriate material selection losses can be minimised, usually to the detriment of cost.

Magnets are also susceptible to eddy current losses as they conduct substantial flux through a large area. The temperature effects due to the eddy currents can also alter the operating point of the magnet. To limit these losses, a magnet can be replaced by a collection of smaller insulated magnets [15], but will then perform less well and increase construction difficulty.

5.2.8 Power Factor

It is an inherent property of the VHM to have a poor power factor [4,16,17]. This is due to the combination of the large self inductances with the high frequency of the machine.

In terms of generation, the reactive power can be simulated by a high reactance in series with the generator emf supplied by the permanent magnets. The magnitude of the reactive power is associated with the amount of energy (E) stored in the airgap and the frequency with which it changes, Eqn. 5.10.

$$Q = 2\omega E = \frac{3\omega L \hat{I}^2}{2} \qquad \text{Eqn. 5.10}$$

A trade off must be made when designing a VHM between flux density (hence shear stress) and reactive power as an increase in shear stress leads to a direct increase in reactive power, Eqn. 5.11, where g is the airgap length [4].

$$Q = \omega g \frac{1}{2\mu_0} \frac{B_{tooth}^2 + B_{slot}^2}{2} \qquad \text{Eqn. 5.11}$$

Power factor can be improved with the addition of capacitors at the machine terminals. This however adds expense and complexity as the significant capacitance values need to vary in conjunction with frequency, voltage and reactive power, which are not constant in variable speed applications. Eqn. 5.12 is used to calculate the capacitance value to correct power factor, where C is the capacitance and V is the output voltage. It is also possible to improve power factor with power electronics or a combination of power electronics and capacitors when the power factor is very low. This may be more suitable for variable speed technology as power electronics are already needed.

$$C = \frac{Q}{\omega V^2} \qquad \text{Eqn. 5.12}$$

5.2.9 Fault Current

The high inductance values of the VHM do provide one advantage. Under fault conditions where high currents flow through the coils, the large inductance limits the magnitude of the fault current. As the current increases so does the rate of change of the current and hence the voltage across the inductor by Eqn. 5.13. From the voltage equation of the synchronous machine equivalent circuit where Z_l is zero, Eqn. 5.14, it can be seen that a high alternating current increases the potential of the coil to the fault and limits the amount of current. By default the inductance adds a degree of safety to the machine and protects the magnets from demagnetisation.

$$v = L\frac{di}{dt} \qquad \text{Eqn. 5.13}$$

$$e = R_c i + L_s \frac{di}{dt} \qquad \text{Eqn. 5.14}$$

5.4 VHM Topologies

The VHM can be constructed in different ways, each having advantages and disadvantages. In this study, three topologies were considered. They are: surface mounted magnet radial flux, buried magnet radial flux and buried magnet axial flux.

5.4.1 Surface Mount Radial Flux VHM

The surface mount VHM (SMVHM) variation has magnets that are fixed to the stator poles between the rotor and the stator i.e., in the airgap. In this case, one magnet provides one magnet pole to the airgap.

The term radial flux is used as the flux that links the stator coils is radial. A radial flux design is comparable to typical machines and thus construction is simplified by using established techniques. For example: the laminations can be laser cut or stamped and simply bolted together as the flux flows in a plane perpendicular to the axle. This lamination orientation will result in the minimisation of all iron losses.

The magnets are mounted inside the airgap and to obtain maximum flux linkage the gap between magnet and rotor should be small. This will in turn produce a substantial attractive force between magnet and rotor that results in difficulties with machine assembly as well as problems associated with adhering the magnets. Assembly problems can be overcome by careful forethought and acceptable processes, but if a magnet should break free the results could be catastrophic.

A SMVHM example is represented in Fig. 5.1 shown previously.

5.4.2 Buried Magnet Radial Flux VHM

Another method of mounting the magnets to the stator of a VHM is to "bury" them within the stator itself and therefore create a buried magnet VHM (BMVHM), Fig. 5.4. This method is advantageous as a technique called flux channelling can be used to provide higher airgap flux densities than is possible in a surface mount design.

Flux channelling works by mounting magnets on steel surfaces so that a north pole faces another north and vice versa which means that two magnets provide one magnet pole to the airgap. By doing this the flux in the airgap should approximately double compared to that of one magnet with the same magnet circuit. When using this method care has to be taken to ensure that saturation does not occur. Increasing the flux and creating stronger fields by

burying the magnets also offers a greater degree of protection against magnet demagnetisation [18]. There are also advantages with respect to improving power factor [17]. Embedding the magnets also reduces the likelihood of a magnet becoming detached and causing the machine to fail.

The disadvantages associated with a BMVHM are mainly due to construction complexities as well as greater emphasis on correct design due to higher flux densities.

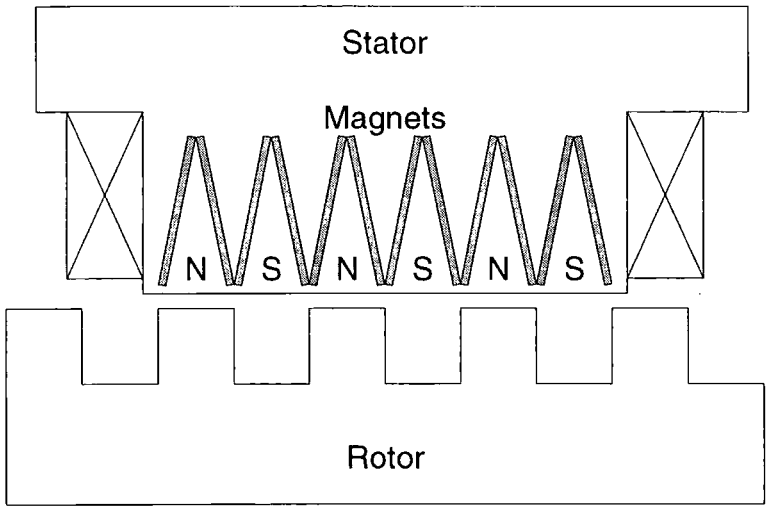

Fig. 5.4: The BMVHM topology studied

5.4.3 Buried Magnet Axial Flux VHM

The axial flux BMVHM (AFVHM) still uses the flux channelling technique but now the plane of the flux that links the stator coils is axial i.e., it flows in a plane parallel to the axle. It has a double-sided rotor to enable a complete flux circuit, Fig. 5.5. As the flux paths have a 3D nature the modelling and hence design of an axial flux machine is more complex. Construction difficulties also increase as the attractive forces due to magnets are not overcome by a solid mounting to the axle, instead a complicated support structure must be designed. The AFVHM does have benefits in terms of torque, eddy current losses in the magnets and shows an affinity to the linear mode of operation.

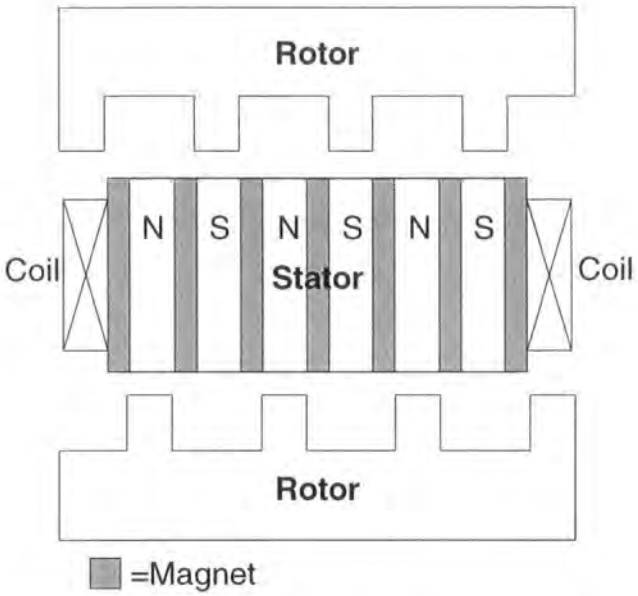

Fig. 5.5: The AFVHM topology studied

6.0 BMVHM Prototype

A prototype BMVHM was designed and built at the University of Durham. The axial length of the final model was reduced by 75% to facilitate ease of construction and testing. The design process was based on simple calculations with the aim of creating a machine for validation purposes, no attempt was made to optimise the design.

6.1 Prototype Parameters

The machine has the specifications as described in Table 6.1 and is schematically shown in Fig. 6.1. The designed rating is 50kW at 1500RPM, but as this prototype is only ¼ the axial length of the rated design and with all things being equal the new rating should be approximately 12.5kW at 1500RPM. The magnetic material used is N30 grade NdFeB with a remnant flux density of 1.12T and coercivity of approximately 800kA/m.

The machine has a two-pole flux distribution and therefore acts as a two-pole machine with higher field angular velocity. The stator consists of six concentrically wound coils of 20 turns, each wound about a tooth containing six magnetic poles.

Each coil turn contains two parallel wires twisted and soldered together at each end. This allows more current to flow per turn without resorting to thicker, unworkable wire. Twisting the wires decreases the long-path eddy current losses as well making the winding process simpler. Coils of same phase are connected in series thus increasing the generated voltage per phase.

Component	Unit	Value
Phase Number		3
Machine Length	mm	24
Stator Bore Inner Diameter	mm	220.4
Stator Bore Outer Diameter	mm	400
Airgap Length	mm	0.2 ±0.1
Number of turns per phase		40
Number of Rotor Teeth		23
Rotor Tooth Width	mm	9.3
Rotor Tooth Length	mm	20
Magnet Length	mm	25
Magnet Width	mm	24
Magnet Depth	mm	2.5
Number of Magnets		72

Table 6.1: Basic machine specifications

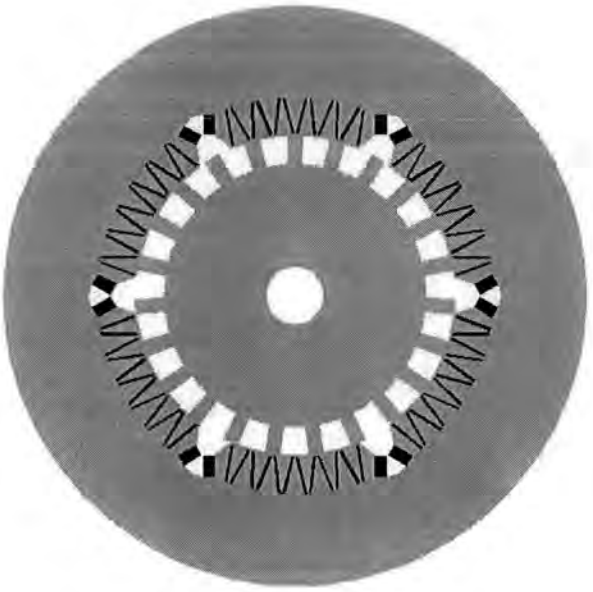

Fig. 6.1: BMVHM prototype

The magnets are arranged in a triangular fashion, with like poles facing each other. This arrangement concentrates the flux so that high flux densities result in the airgap, Fig.6.2.

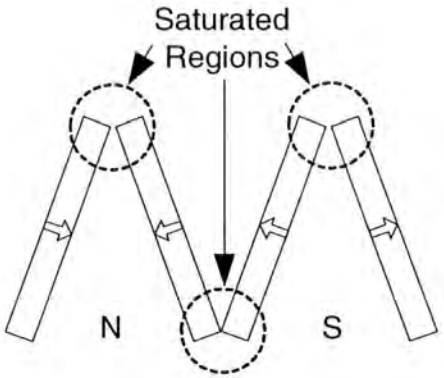

Fig. 6.2: Stator magnet arrangement

Mounting the magnets within the stator core was simplified by pre-cutting slots for the magnets to slide into. As the slots are closed by thin bridges, leakage flux will pass and cause the bridges to saturate as highlighted in Fig. 6.3 by the red regions. As these parts are small and the construction greatly simplified by their inclusion, the saturation effects are tolerated.

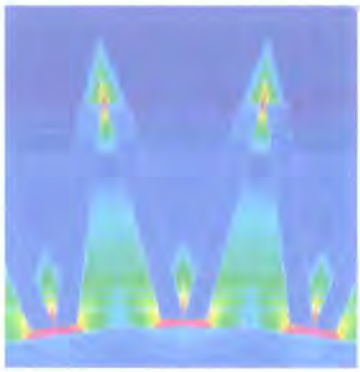

Fig. 6.3: BMVHM leakage flux density plot

Construction of the prototype is relatively simple due to radial and circumferential flux paths allowing all laminations to be bolted together. Assembly is straight forward as the rotor can be lowered into place with the shaft and bearing providing support and preventing attraction of the rotor to the stator caused by the interaction of steel and magnets. The machine is mounted on a test rig that incorporates an 8 pole 5kW induction motor with variable speed control via a PWM inverter drive. The test machine was coupled to the motor so that open and short circuit tests could be conducted.

Photographs of the BMVHM are contained in Appendix G.

6.2 Results

Various tests were performed at low speeds where the values for open circuit voltage (V_{oc}) and short circuit current (I_{sc}) were determined. Due to the small size of the machine and load banks available, accurate load tests were not feasible. For testing purposes the prototype was coupled to the eight-pole induction motor. The top speed for the tests was 750RPM. To record results the output from the star connected BMVHM was fed through a 3 phase power analyser. Some static rotor tests were also possible and provided values of static torque (τ), coil resistance (R_c), self and mutual inductance (L_s, L_m). All of these values can be used to describe the machine through the equivalent circuit.

6.2.1 Open and Short Circuit Tests

The open circuit voltage, which is measured at the machine terminals, is a measure of the emf produced by the windings. To measure this a voltmeter is used to record the rms phase voltage and readings are taken for various machine speeds which are recorded with the use of a tachometer. Another useful measurement is that of the short circuit current. Using an ammeter, the current at a 3-phase short circuit is measured for one phase. In

order to gain more meaningful information from these two values, the internal resistance of the machine must also be measured. In this instance the resistance is small and the resistance of the meters connection points significant, so for greater accuracy the four point method was used.

Eqn. 6.1, is used to calculate the generated frequency. For this prototype to operate at 50Hz, a rotational speed of 130RPM is required as the machine has 23 teeth. The machine did have a very large temperature increase when left running at higher speeds and is due to the large iron losses which increase approximately with the square of frequency. For grid connection, without electronic frequency control, the normal operating speed of approximately 130RPM does not induce high iron losses.

$$f = ToothNumber * \frac{RPM}{60} \qquad \text{Eqn. 6.1}$$

As expected, the emf exhibits a linear relationship with speed, Fig. 6.4. There is a slight deviation from linearity at higher speeds. This is not related to saturation but is attributable to temperature effects. The magnets exhibit a temperature increase with speed due to losses within the magnets and thermal conduction resulting from the iron losses of surrounding material. This increase causes a reversible loss of remnance, provided that the temperature does not exceed about 150°C, and thus reduces the flux linkage and hence emf. For the N30 grade of NdFeB used, B_r decreases by 0.12%/°C, Appendix A.

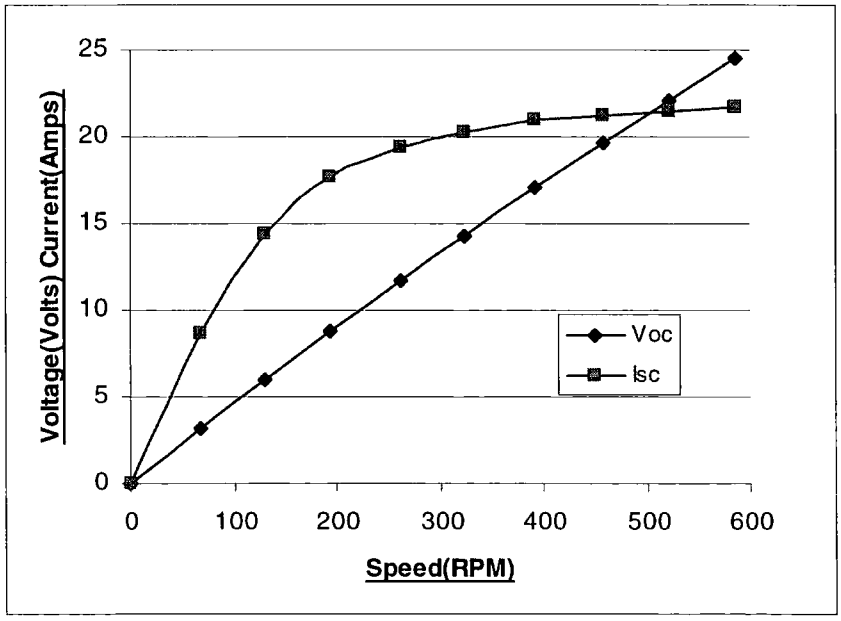

Fig. 6.4: BMVHM open circuit and short circuit characteristics

The short circuit current initially exhibits a linear relationship when the resistance is predominant and the current is described by V/R. At higher speeds I_{sc} is affected by the high reactance of the VHM, the knee represents the transition from resistance to reactance dependency. Inductance limits the amount of current that flows through the circuit and hence the output current will find an upper limit.

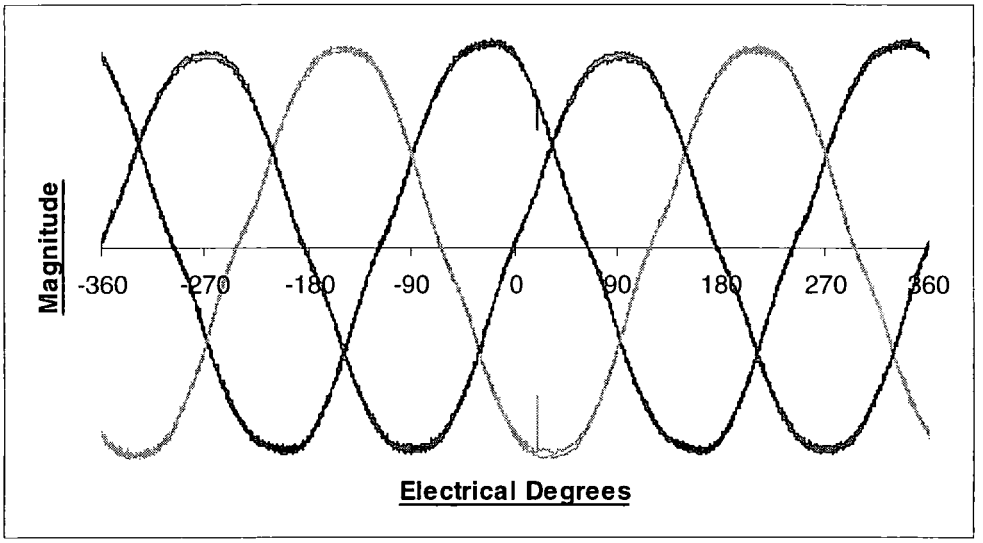

Fig. 6.5: BMVHM 3 phase emf distribution

The 3 phase emf was captured on a storage oscilloscope and displayed characteristics very close to that of a 3 phase sine wave, Fig. 6.5. A simple harmonic analysis shows that the fundamental is far more significant that any other harmonic.

From FEA the airgap flux density distribution is as shown in Fig. 6.6. This curve represents the flux density at a point in the airgap midway between rotor and stator and in the centre of a magnet pole. The distribution is achieved by moving the rotor past the point for one electrical period and gives an indication of the flux variation. The distribution approximates a sinusoid for the first half of the cycle, the second half has essentially constant flux density as it is in the unaligned position. At this point the adjacent magnets conduct flux with opposite polarity. This distribution is for a point and the induced emf approximates a sinusoid more closely as it is related to the flux density over a larger area.

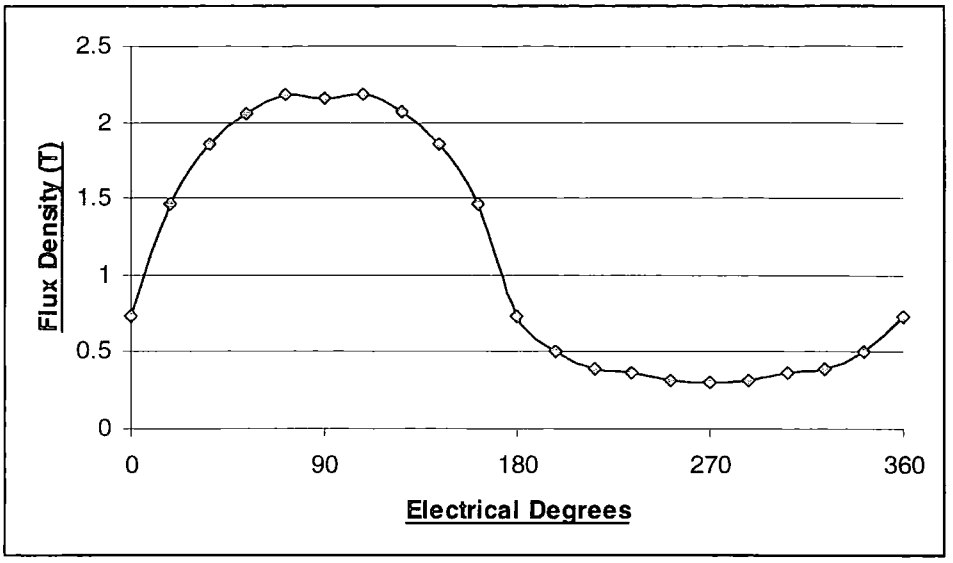

Fig. 6.6: Airgap flux density distribution

One concern with the use of permanent magnet machines is the effect of cogging and reluctance torques. These are the torques produced by the tendency of the rotor to align in a position of minimum reluctance. This attraction is reinforced in the VHM by the large gradients of flux density due to using narrow teeth and magnets. This torque superimposes itself onto the operating torque and adds ripple which can transfer harmonic components to the generated current and induce acoustic noise [18]. The BMVHM exhibits some cogging torque but as the number of magnet poles and teeth is high and interact in a vernier fashion, the cogging torque components should mutually cancel in a perfectly constructed machine.

6.2.2 Static Torque Tests

To measure static torque, DC currents are applied to the coils of the machine in such a manner that a field is created that models that of 3 phase system when one phase is at a maximum, Fig. 6.7. By attaching a lever arm of known length to the shaft and hanging a set of weights off the end, the torque at various levels of current can be determined. The results for these tests are shown in Fig. 6.8. Using Eqn.6.2, at a torque of 63Nm a mean shear stress value of 35kN/m^2 is calculated. This mean value is not the maximum for the machine and from FEA the threshold value approaches 70kN/m^2.

$$\hat{\sigma} = \frac{\tau}{\pi r^2 l} \qquad \text{Eqn. 6.2}$$

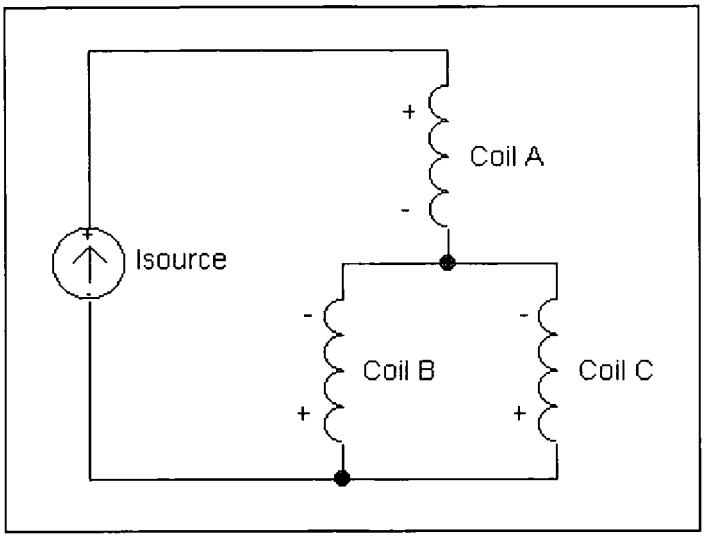

Fig. 6.7: Coil connection for static torque tests

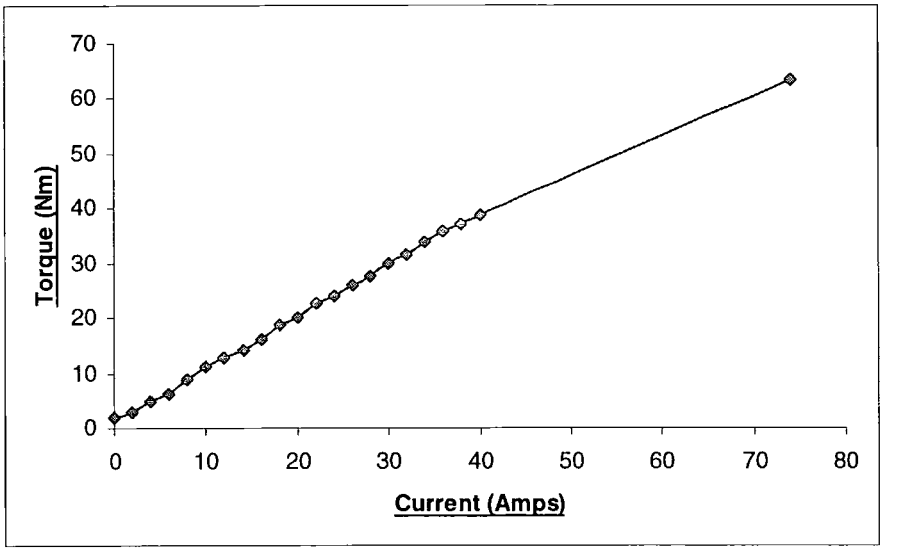

Fig. 6.8: Measured static torque versus current characteristics

The threshold value for shear stress is determined by saturation of the iron core. When saturation begins, the magnetic loading no longer increases and the torque remains constant. To saturate the iron of the test machine would need a current of approximately 100A. This is impractical due to the difficulty of accessing such high currents and using them for any sustained period of time at values well above the machine rating. To be able to test the machine at the highest current value of 74A required two heavy-duty car batteries in parallel as a supply. All measurements had to be taken quickly due to the thermal limitations of the coils.

It can be seen that the machine has a potentially high torque capability but this cannot be utilised within the prototype as the coil current ratings are too low.

6.2.3 Inductance Tests

To be able to model a machine adequately, the synchronous inductance at the machine terminals is desired. This can be calculated while under operating conditions with the use of the frequency, V_{oc}, I_{sc} and R_c by Eqn. 6.3. The measured phase inductance was approximately 0.8mH per phase as shown in Fig. 6.9.

$$Z = \frac{V_{oc}}{I_{sc}} = \sqrt{R_c^2 + X^2} = \sqrt{R_c^2 + (\omega L)^2} \qquad \text{Eqn. 6.3}$$

Solving for L:

$$L = \frac{\sqrt{\left(\frac{V_{oc}}{I_{sc}}\right)^2 - R_c^2}}{\omega} \qquad \text{Eqn. 6.4}$$

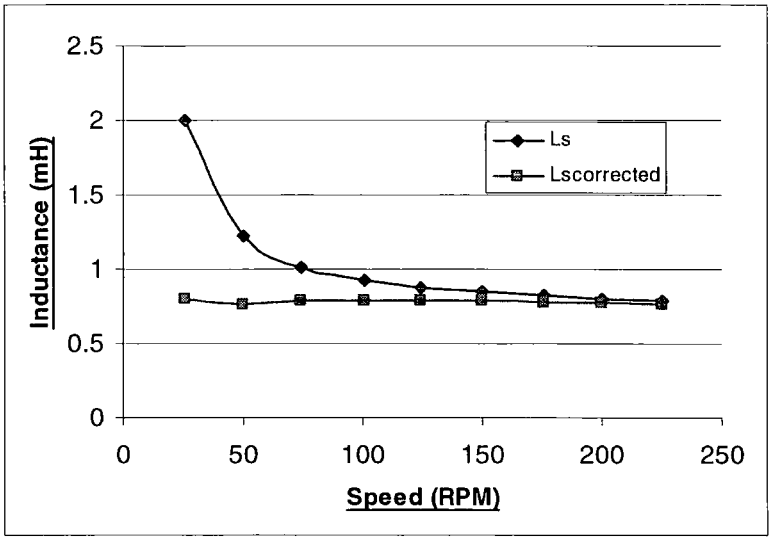

Fig. 6.9: Measured synchronous inductance

The apparent inductance varies in the low speed region as at this point the value of resistance is significant compared to that of reactance. Any error in resistance measurement results in a deviation of inductance at low speed. It is likely that the measured resistance was lower than that during operation due to the temperature rise of the machine from previous tests and added resistance due to cabling from the test point to the

machine terminals. Adding an error of +100% to the resistance measurements, which is quite probable, results in a much more linear characteristic, Fig. 6.9.

Self and mutual inductances can also be measured. To determine self inductance per phase an inductance meter is used. Mutual inductance is found by passing a known alternating current (I_1) at known frequency into one phase and measuring the resulting emf generated in another (E_2) using Eqn. 6.5 to find the mutual inductance to the original phase. Measurement values resulted in a self inductance of 0.55mH per phase and a total mutual inductance of 0.13mH resulting in 0.68mH total inductance which does not include leakage inductance and is comparable to the open and short circuit results.

$$L_{M1-2} = \frac{E_2}{\omega I_1} \qquad \text{Eqn. 6.5}$$

6.3 Results Comparison

6.3.1 FEA

Measurements from FEA and tests are compared and results are displayed in Fig. 6.10 and Fig. 6.11. The general trend of results between FEA and measurement is fairly similar and is an indication that the machine is performing as expected. Unfortunately the magnitudes of the variables are comparable but not identical. The first explanation for this discrepancy is that the FEA software used only calculates for 2 dimensions. As the machine is 24mm in axial depth two sides of each magnet are exposed to end leakage which is unaccounted for by the FEA package, Fig. 6.12. As a proportion of axial length this turns out to be significant. Other factors include: differences in material property settings, parameter values and end winding leakage. The end result is that the FEA grossly over predicts the machine emf, inductance and torque.

One method of improving FEA accuracy is to combine FEA results with external calculations. Eqn. 6.6 is one method of quantifying the flux leakage in the third dimension due to the magnets, where the radii correspond to Fig. 6.12. Derivation of Eqn. 6.6 is contained in Appendix C. The procedure provides an approximate value for the leakage at each side of each magnet and can be used to find the total leakage per phase. Now the leakage flux can be subtracted from the FEA results to provide a more accurate representation. The result of including this calculated value for leakage flux is shown in Fig. 6.10.

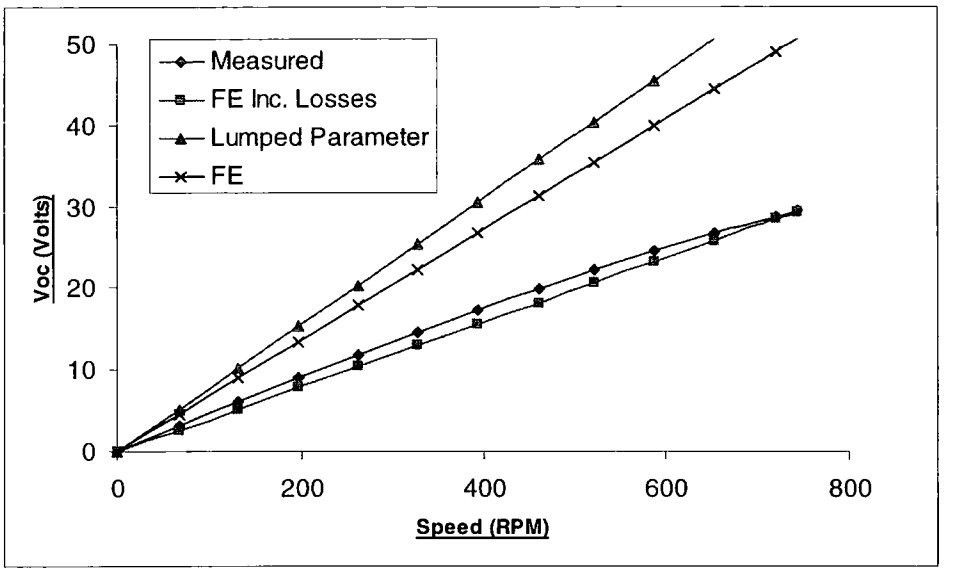

Fig. 6.10: FEA, LP and measured results comparison for V_{oc}

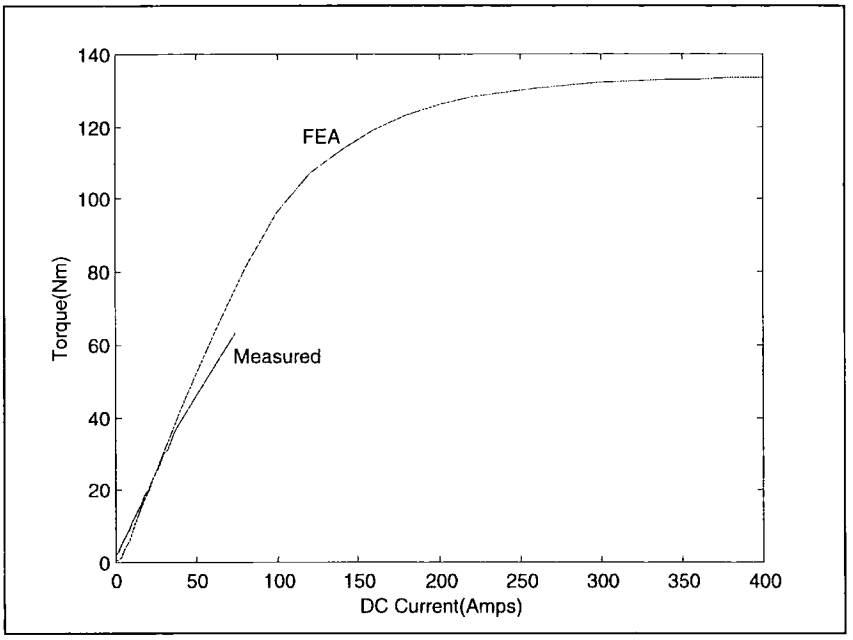

Fig. 6.11: FEA and measured results comparison for torque

$$\phi_l = \frac{M_l \mu I}{\pi}[\ln(r_2) - \ln(r_1)] \qquad \text{Eqn. 6.6}$$

Using this calculation shows that approximately 20% of the total flux for one phase is lost as end leakage flux.

The per phase inductance calculated from FEA is 1.8mH (Appendix D), this value does not include the 3D flux leakage but does include leakage inductance. By reducing the flux

values used by 20% the resulting inductance value is 1.4mH which when compared to the measured results is more accurate.

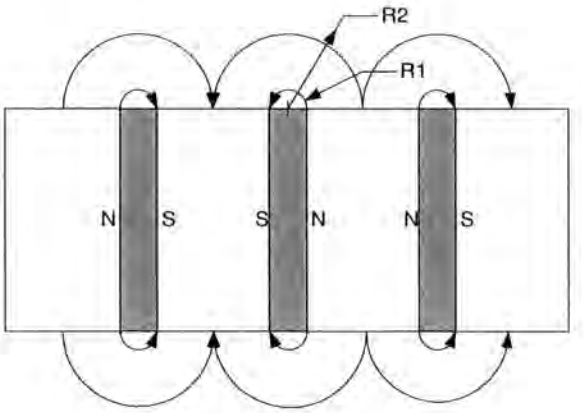

Fig. 6.12: End leakage flux

6.3.2 Lumped Parameter

Lumped parameter analysis is not readily applied to the BMVHM because of saturation in the iron bridges. The analysis was conducted in a modified form and provided some interesting results showing good accuracy when appropriate measures are taken to include features such as leakage and saturation.

Magnet leakage flux was calculated with Eqn. 6.6, while the leakage flux between magnets was recalculated. To define this leakage some assumptions were used. As the magnets are strong and the flux paths between them are small it is feasible to assume that the leakage paths are in saturation, a value of 2T can be used as an estimate for mild steel. Then by knowing the area that the flux flows, A_{leak}, Eqn. 6.7 is used to define the flux magnitude in each leakage path. These values are summed per magnet and provide a reasonable estimate. FEA does not require this prediction as this leakage lies in a plane that the FEA software solves for.

$$\sigma_l = \frac{B_{sat}}{A_{leak}} \qquad \text{Eqn. 6.7}$$

As expected, the lumped parameter results are not very close to the measured values, Fig. 6.10. It is interesting to note that the results can be made to be more accurate by manipulating input values to the limits of their tolerances. This is not useful with respect to design but does show that lumped parameter accuracy can be improved if precise input parameters and material properties are available.

7.0 Axial Flux VHM Prototype

Using the results and information gained from the BMVHM, another VHM topology, the axial flux VHM (AFVHM) was designed, built and tested. This topology may improve on the shear stress and iron losses of the BMVHM and hence a prototype was built to confirm this expectation.

7.1 Qualities

Despite being a different topology the concept of the AFVHM was derived from the BMVHM and incorporates many of its advantages. The best way to describe this new topology is to start with the BMVHM and use a visualisation process.

If the BMVHM were cut from the centre to the outer circumference it could be unfolded to form a linear machine, Fig. 7.1.a. Mirror this machine along the stator, (not including the stator back iron, which becomes redundant in the final machine) and displace one rotor by half a tooth pitch, Fig. 7.1.b. As some of the iron is not conducting flux the magnets can now be rearranged as in Fig. 7.1.c. To turn this linear version into a rotating machine, each end of the machine is simply bent out of the plane of the paper so that they meet.

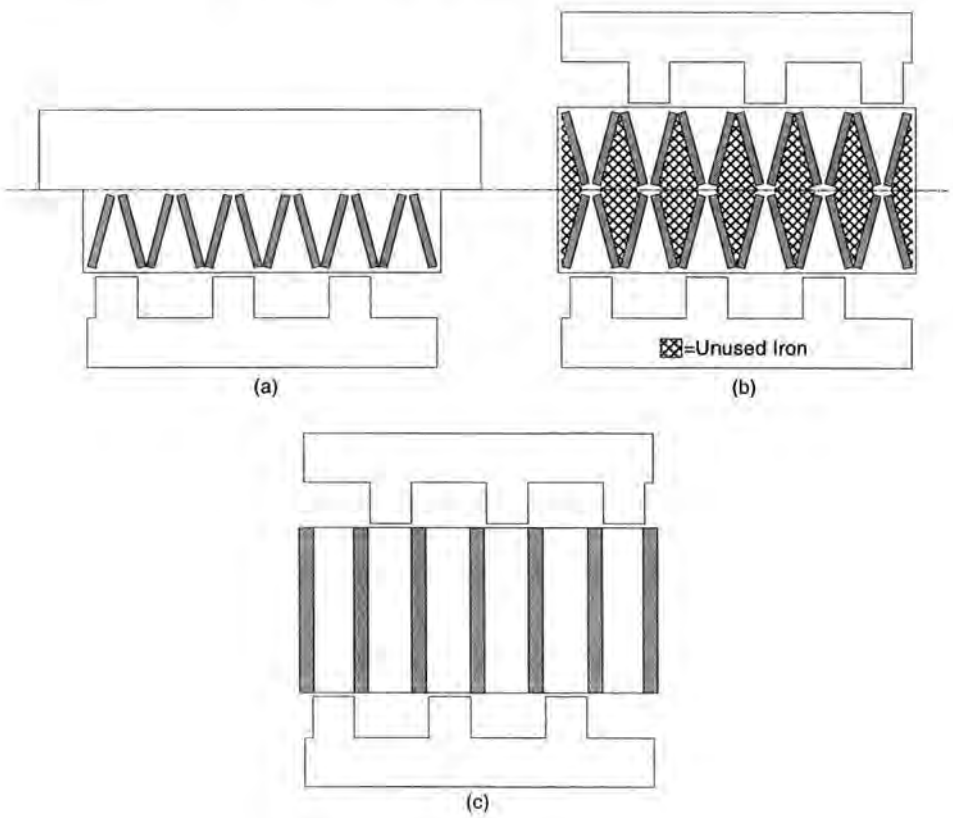

Fig. 7.1: Development of the AFVHM from the BMVHM

If the rotors were not displaced relative to each other, losses would develop in the magnets. The magnets operating up and down their recoil lines as the rotor moves from an unaligned to an aligned position cause these losses. This changing flux density induces eddy current losses within the magnets. Arranging the magnets parallel to the rotor axis and displacing the rotors apart by half a tooth pitch can gain a significant benefit.

Examination of Fig. 7.2 shows that through one rotor displacement of half a tooth pitch, the pulsations of flux in each airgap are in antiphase. Therefore the magnitude of flux through each magnet does not significantly change. If there is no changing flux through the magnet there can't be any eddy current losses within the magnet itself or in the locally surrounding steel.

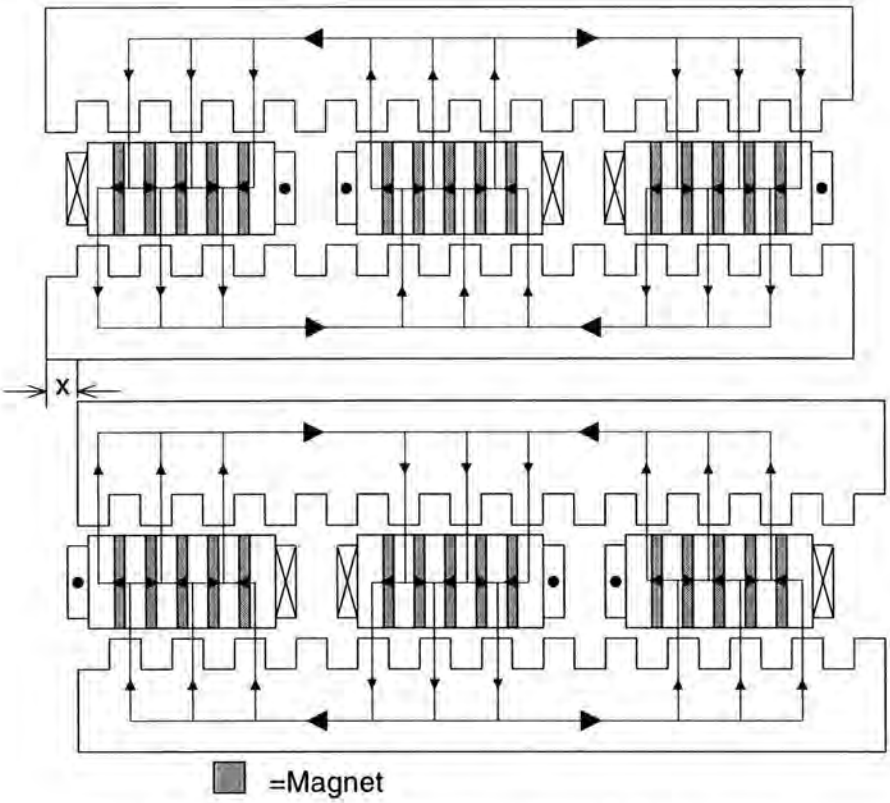

Fig. 7.2: Unidirectional flux flow through the magnets

Displacing the rotors also causes each magnet to carry flux continuously, resulting in the magnetic material being used more efficiently and at a higher loading with less leakage [2], hence improving the magnetic gearing ratio.

7.2 Design Process

Once the basic topology of the AFVHM is decided, the design process can begin. Two design methods were used in combination. The first method used lumped parameter analysis and the second FEA. Before any complex design commences, some basic parameters must be decided as a reference or starting point. These may be cost, size, power or simply a design that fits the components that are available e.g. magnets. In this case the machine was designed around some available NdFeB N30 magnets with a general machine size in mind.

7.2.1 Lumped Parameter

Lumped parameter analysis, despite being rather approximate is still extremely useful as a starting point because of its speed and simplicity. From the general machine topology a basic magnetic equivalent circuit can be deduced, Fig. 7.3. It should be noted that the circuit depicted is a repeating unit that is assumed to repeat in both directions towards infinity. This assumption makes the calculation of specific node potentials simpler. By reducing this circuit using network analysis, the flux in the airgap for full rotor alignment and misalignment can be calculated, the sum of which defines the net flux for the unit, Appendix E. The total flux is simply a summation of the flux for the number of units per phase.

Other properties can also be derived by removing the magnets form the equivalent circuit and adding an external mmf due to the coil.

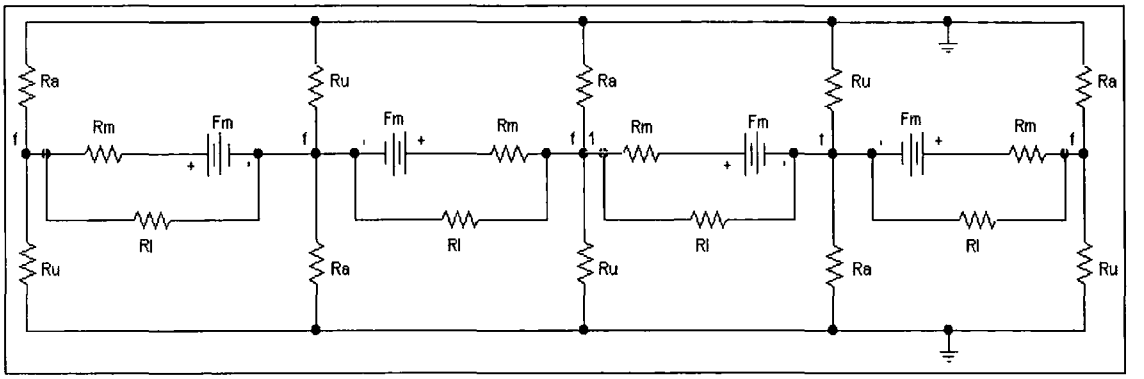

Fig. 7.3: AFVHM lumped parameter equivalent circuit

7.2.2 FEA

The machine dimensions derived from the lumped parameter analysis are used to draw a FEA model. The FEA software can now be used iteratively to refine the values until a

design that optimises and fits the desired specifications is found. At this point more in depth FEA can be resumed and characteristics predicted.

As the AFVHM is inherently 3D, the model used in the 2D FEA software must be altered from the desired topology and the inaccuracies acknowledged. The simplest way to model the AFVHM in 2D software is to convert the machine from round to linear. Fig. 7.4 depicts the preliminary FEA model, this model represents half of the total machine length and was used to increase accuracy as high node densities could be achieved. The error associated with this is that some segments are rectangular and not tapered due to the curvature and will then have differing flux densities in the radial direction that are not modelled. Nearly all the variables were alterable in the FEA model which allows for in-depth design assessment.

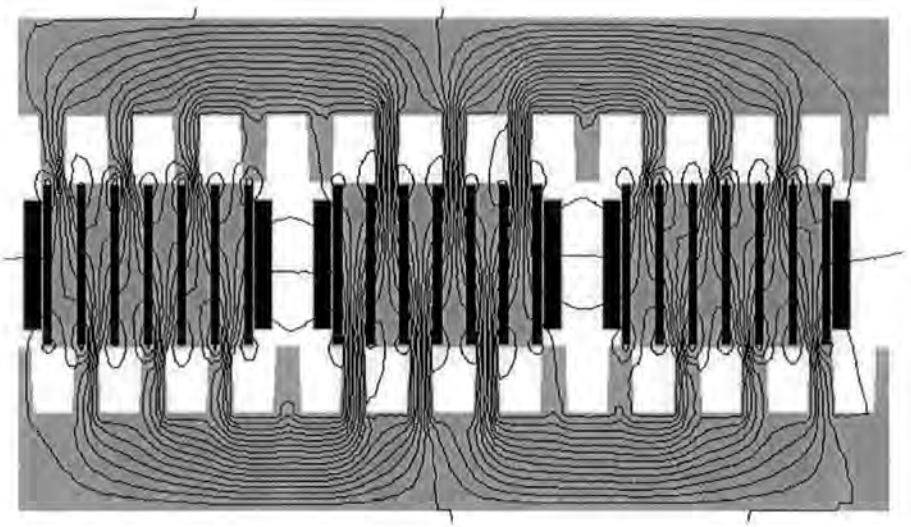

Fig. 7.4: FEA model for the AFVHM

To minimise the error, the values that were used from the FEA were the values that represented dimensions of the inner radius of the machine. By considering this, the design was finalised at slightly higher than desired flux densities as the increasing tapering of the teeth will decrease the overall tooth flux density where saturation is most likely.

7.2.3 Coils

The coil design is set by the required output voltage at the rated speed range. This voltage may be limited by the rating of the power electronics, safety factors or in this case by the peak voltage of the load. The load motor of the Ward Leonard rig has a rated voltage of $400V_{dc}$. It is therefore the maximum permissible voltage of the rectified AC output from

the test machine. The conversion to calculate 3 phase AC voltage to rectified 3 phase voltage with a diode bridge full wave rectifier is shown by Eqn. 7.1 [19].

$$V_{dc} = \frac{3\sqrt{2}}{\pi} V_{l-l} = \frac{3\sqrt{6}}{\pi} V_{l-n} \qquad \text{Eqn. 7.1}$$

7.3 Prototype Parameters

The final parameters for the AFVHM are displayed in Table 7.1. The output is 3 phase and the stator consists of 6 coils, each wound on a single stator block containing 6 magnets and 6 steel pieces. Each phase winding comprises two coils in series.

Component	Unit	Value
Machine Active Length	mm	30
Stator Bore Inner Diameter	mm	300
Stator Bore Outer Diameter	mm	360
Airgap Length	mm	2±0.5
Number of turns per phase		160
Number of Rotor Teeth		26
Rotor Tooth Width	mm	9.3
Rotor Tooth Length	mm	20
Magnet Length	mm	50
Magnet Width	mm	30
Magnet Depth	mm	6
Number of Magnets		36

Table 7.1: Basic machine specifications

The stator blocks are not symmetrical as one end does not have a magnet attached. From the FEA analysis it was found that considerable leakage flux exists between the end magnets for adjacent stator blocks, Fig. 7.5.a. As adjacent end magnets are facing north to south a convenient leakage path between stator blocks and through rotor teeth is created. By leaving off the same end magnet for each stator block, adjacent blocks are now facing north to north and the leakage flux is minimised, Fig. 7.5.b. This can be done with minimal effect as the magnet has no bearing on the magnet pole pitch, which is defined by the width of the steel piece between magnets. The removal of one magnet also creates a greater distance between stator blocks and hence the winding area can be increased. One disadvantage is that the total flux linkage and airgap distribution is distorted, but as all the blocks have the same magnet missing the net effects are balanced.

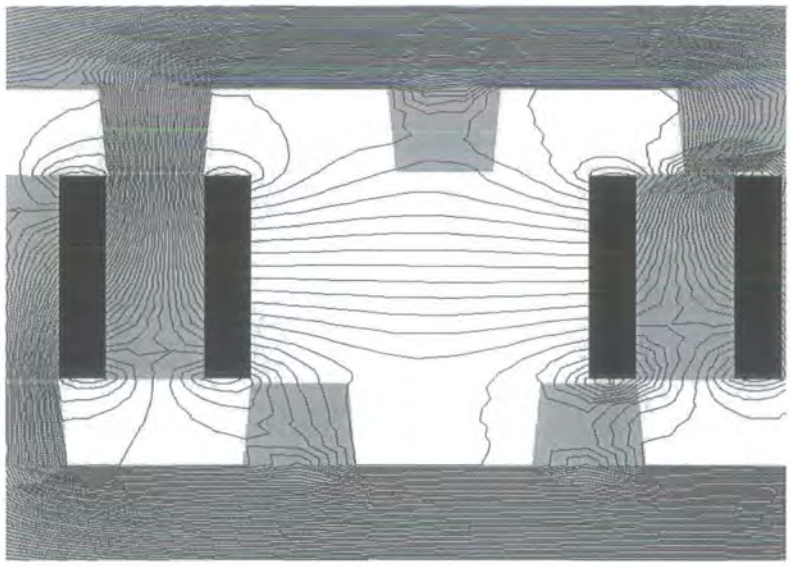

(a)

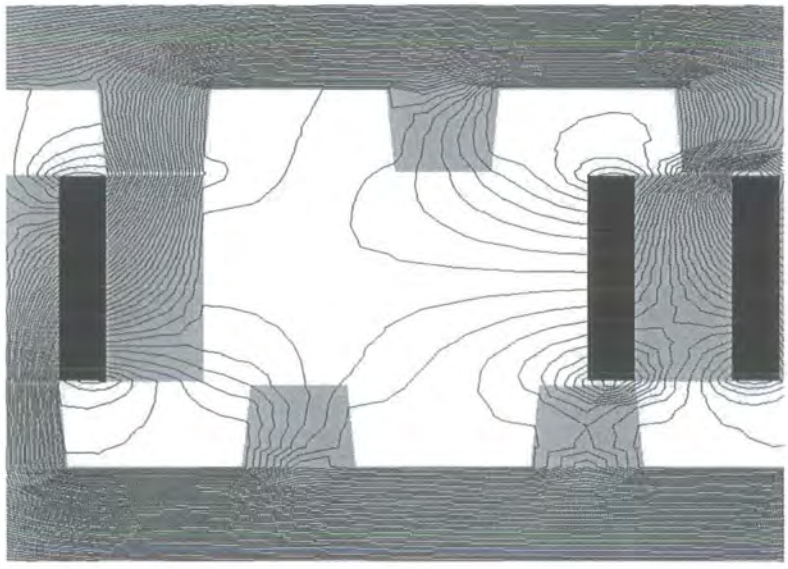

(b)

Fig. 7.5: Leakage reduction by omitting a magnet

Each coil has 80 turns of conductor formed of three parallel 1mm diameter wires, the coils are connected in series and thus provide 160 turns per phase. The design process that leads to these values is contained in Appendix F.

7.4 Construction

The construction of an AFVHM is rather complex and can be separated into three aspects: the rotor, stator and assembly. A rotating rather than linear machine was preferred as it was thought that the difficulties associated with building a linear test rig were excessive. However, the rotary design also adds other complexities associated with lamination

assembly and using magnets of rectangular shape in a round stator. Construction difficulties associated with a prototype are always numerous and much can be learned to improve processes for a commercially built design. Fig. 7.6, depicts a cross sectional view of the prototype AFVHM, photographs are contained in Appendix G.

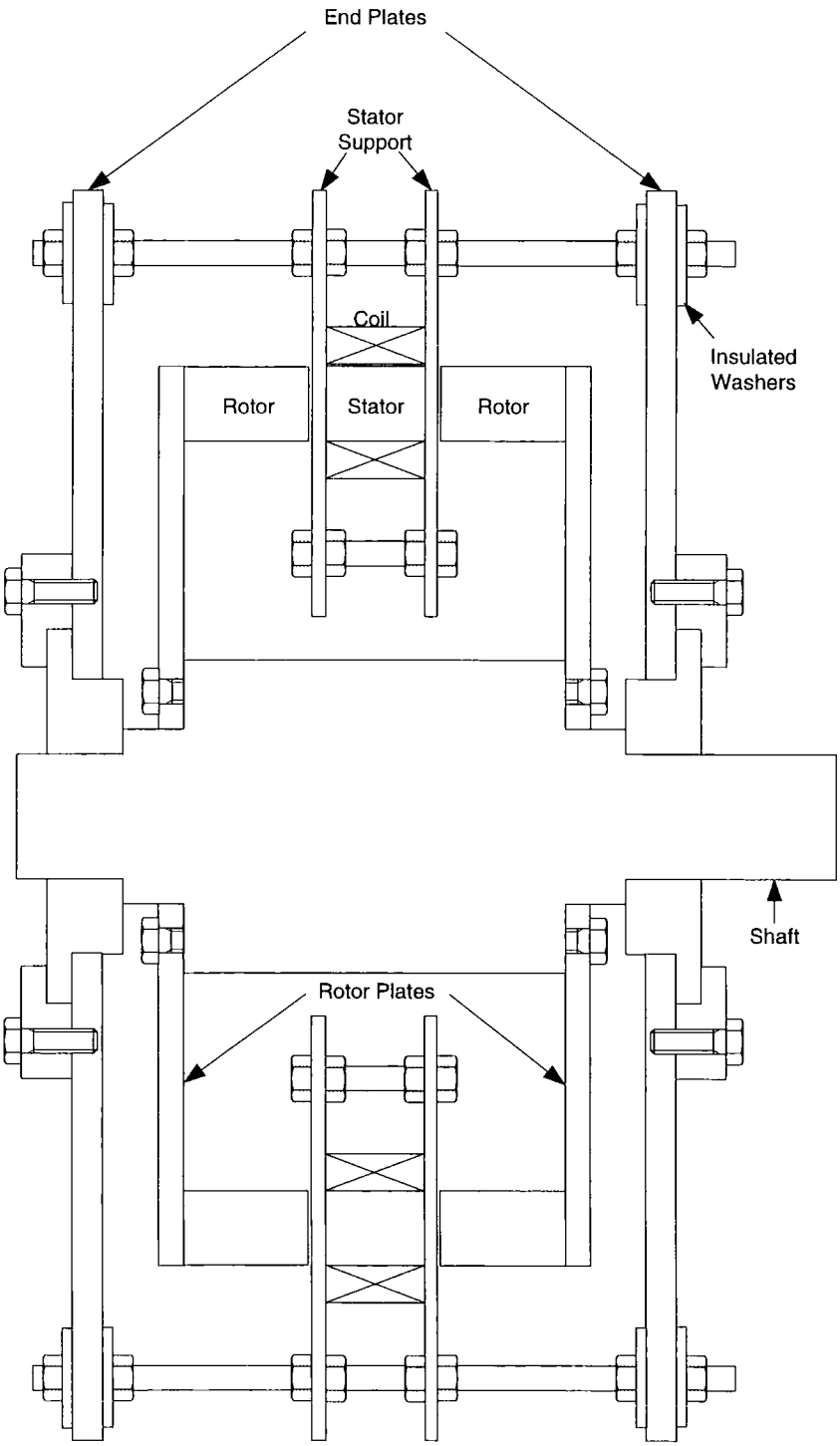

Fig. 7.6: A cross section of the AFVHM prototype

7.4.1 Rotor

Rotor flux paths lie on cylinders concentric with the axis. The rotor should therefore be laminated as a set of concentric cylinders or, more conveniently, a spiral. The addition of teeth now adds more complexity to the rotor construction. In order to reduce difficulty an ingenious method was devised.

The rotor was built using laminated spirally wound toroidal cores, this was achieved by milling 26 20mm deep equidistant slots in the toroid to form the rotor teeth. The laminations remained intact as they were bonded together with epoxy during construction. The slots were milled using a dividing head, each slot was created in a single operation forming parallel sides. Although parallel-sided slots are not ideal magnetically, this error is small and justified by the economy of the operation, also as edges of the rotor and stator teeth do not align perfectly it is possible that residual cogging torques are reduced as a result.

7.4.2 Stator

Like the rotor, the stator construction is difficult as the flux paths lie on cylindrical surfaces and the iron teeth should be laminated accordingly. However, the tangential component of the flux is steady so it would be permissible to only use laminations in the radial plane, but this freedom was not found to offer any benefit. Once again the toroidal cores provided this function. In this case, the toroids were cut into segments that matched, as closely as possible, the dimensions of the steel stator segments, Fig. 7.7.

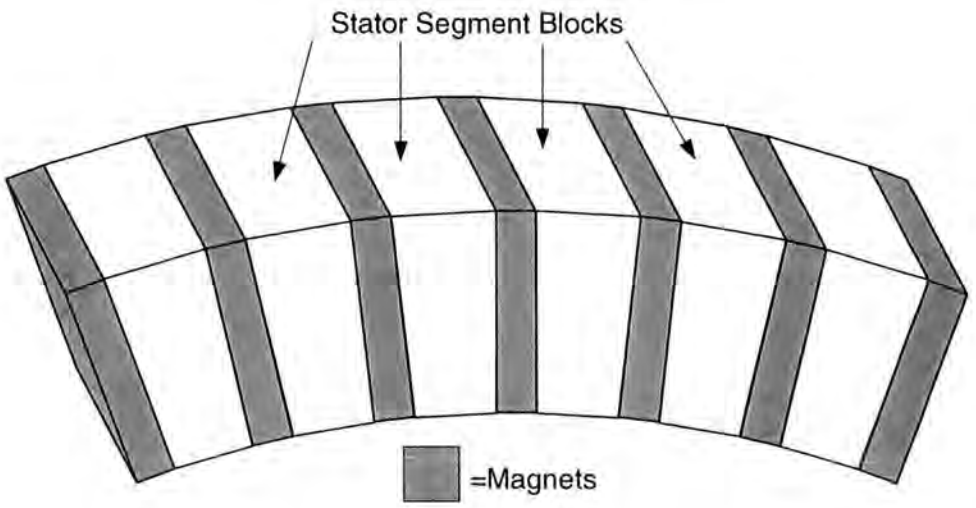

Fig. 7.7: Stator block

Each magnet in the stator repels the next as is required by the flux concentration principal. Unlike the BMVHM the magnets are not encased by the stator and hence have to be glued to the steel pieces. The repelling fields also act as to separate the upper and lower steel piece laminations thus requiring some tedious construction procedures.

As the stator contains magnets, there are high attractive forces between it and the rotor. The attraction is significantly reduced by using a two-sided rotor as the forces on the stator act in opposite directions hence producing a smaller net force. By rotating the rotor, a pulsed net force will still act due to the reaction of tooth to magnet pole. To keep the airgap constant, the stator blocks must be supported, particularly in the axial direction. Fig. 7.8 shows the supporting structure designed to hold the stator blocks. The rotor will be equally attracted to the stator but the rotor construction can be made far more rigid and is not of major concern.

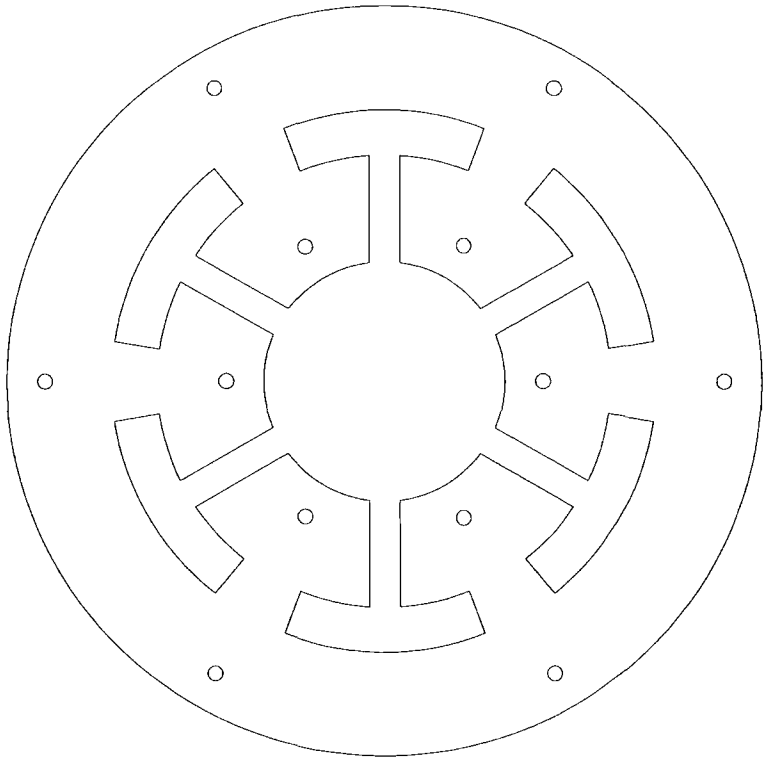

Fig. 7.8: The aluminium stator support

To ensure that the supporting material doesn't provide a low reluctance path for useful flux it must be made from a non-magnetic material. For this application aluminium was used because of its availability, weight, strength and low permeability. To retain the stator blocks within the aluminium, a large amount of heated epoxy was forced into the gaps

between block and aluminium. The aluminium support structure is held by the machine end plates which are mounted to a rigid base.

One precaution that must be taken with the aluminium is that there must not be a conducting path about the stator block. If there is, the alternating flux flowing through the stator will induce currents that will flow around the block and incur I^2R losses. To avoid this, slots that break the circuit have been cut from the inner diameter of the support to the stator slots. It is also necessary to insulate areas where the current may find an alternative path e.g., bolts and milled stator surfaces that touch the stator blocks.

7.4.3 Assembly

Typically, assembly of machines containing permanent magnets is difficult as the attractive forces are large and unstable. A radial-flux machine simplifies assembly as the rotor can be inserted into the machine using the axle in the bearing as a guiding support. The AFVHM cannot be assembled in this manner due to the double-sided nature and stator construction. Using FEA a prediction of the force attracting the stator block to the rotor is calculated with Eqn. 7.2 for the Maxwell stress [20]. Where B is the average flux density in the airgap over the length desired.

$$M_s = \frac{B^2}{2\mu_0} \qquad \text{Eqn. 7.2}$$

Eqn. 7.3 translates stress into force, where A is the area that the force acts upon.

$$F = M_s A \qquad \text{Eqn. 7.3}$$

From FEA, the estimated force for one rotor is 700N for an airgap of 2mm. As there is an equal and opposite force for the other side the net force should be zero. This is only true if there is perfect dimensional and material symmetry on either side of the machine. Each stator block is tangentially asymmetrical and so the reluctances between the stator and each rotor are different and change with rotor position. The forces are therefore different and a net force will be exerted on each block. The direction and magnitude of this force is likely to change with rotor position and hence a ripple torque and vibration are expected. Limitations due to construction may also place limits on the size of the airgap. The stator support was designed to withstand large forces so that a safety margin is introduced.

After construction it was noticed that the airgap was not uniform.. This is due to the construction of both the stator and the rotor. As a result the airgap varies with the position of the rotor and hence causes unusual vibrations. Originally the machine was designed for an airgap of 1mm but during construction it was thought best to increase this to 2mm so that the attractive forces are reduced and the construction simplified. This results in the machine running at values lower than designed for.

7.5 Testing

The testing processes used for the AFVHM are equivalent to those used on the BMVHM. In this case, on load tests are feasible because of two differences: the AFVHM prototype has a higher power rating and a new Ward Leonard test rig has been built and commissioned.

The Ward Leonard testing rig has great advantages over simply driving a test machine and dumping the output power in resistor banks. The Ward Leonard set up is also more efficient as the power is recycled and used to feed the drive machine. Machines of varying sizes can also be tested on the same rig. A schematic for the test rig is contained in Fig. 7.9.

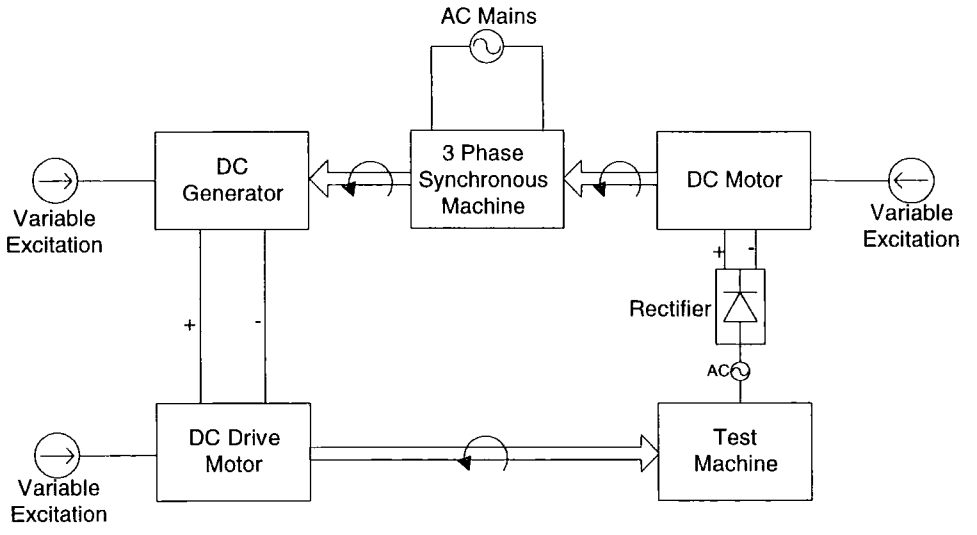

Fig. 7.9: Ward Leonard test rig schematic.

Operation of the Ward Leonard system is as follows. A synchronous machine directly drives a DC generator at synchronous speed. The output from the generator is fed to the DC drive motor, which rotates the test machine. Both the DC generator and drive motor

have variable excitation, which enables variable speed of the drive motor and hence test machine. All VHMs tested have a sinusoidal emf and therefore a rectifier is needed so that the output can be fed to another DC motor on the same shaft as the dc generator. This motor drives and reduces the load on the AC machine. In this way, the power is circulated through the circuit, with the mains supplying only the system losses, making the system efficient. The DC motor also has variable excitation which when reduced allows a simulated load to be placed on the test machine. A torque transducer is incorporated in the coupling between the test machine and drive motor and provides a measure of the input torque. Using a combination of controls a complete range of tests can be completed.

7.6 Results

Open and short circuit tests were conducted and the same procedures as with the BMVHM used. Due to time constraints the Ward Leonard test rig could not be used and was instead substituted with a resistive load bank. In this case, the generator was coupled to a 10kW DC drive motor. The maximum test speed was limited to 200RPM as above this speed the vibrations caused a resonance effect with the machine mounting frame.

7.6.1 Open and Short Circuit Tests

The open and short circuit results are depicted in Fig. 7.10 and are as expected. From these characteristics it is possible for the machine to produce 1150W at 200RPM. This corresponds to a torque of 61Nm and a mean shear stress of 11.9kN/m^2. These values are not extraordinary but are encouraging when the large airgap is considered, especially since the VHM is dependant on a small airgap. The region where I_{sc} is a function of resistance is not approachable in this case as the machine is not easily rotated at the low speed necessary.

Fig. 7.11 depicts the 3 phase emfs for the AFVHM and shows that the peak voltages for each phase are not equal. After using a Gauss metre to measure the polarity of each stator block it was found that one of the magnets was inadvertently placed with incorrect polarity during one of the machine rebuilds. This results in varying phase voltages and will also induce currents in the neutral point when star connected feeding a balanced load with a four-wire circuit. It was also noticed that the peak voltage per phase oscillates with rotor position, this is solely attributable to the varying airgap length which again is a result of construction difficulty.

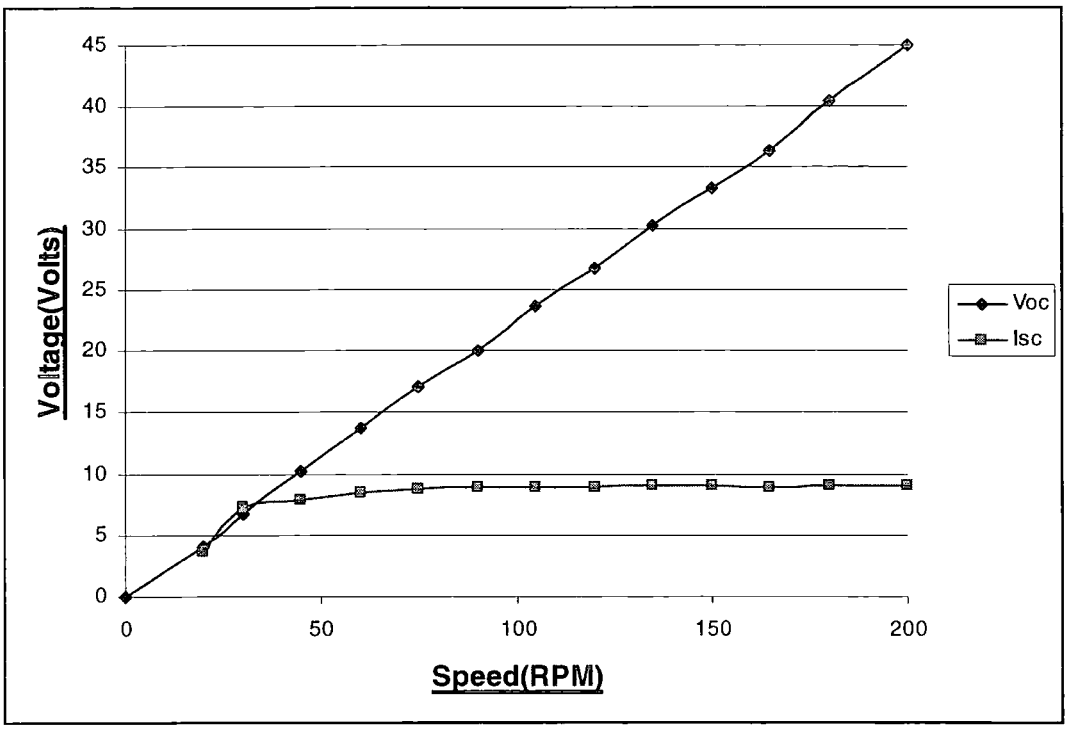

Fig. 7.10: AFVHM open circuit and short circuit characteristics

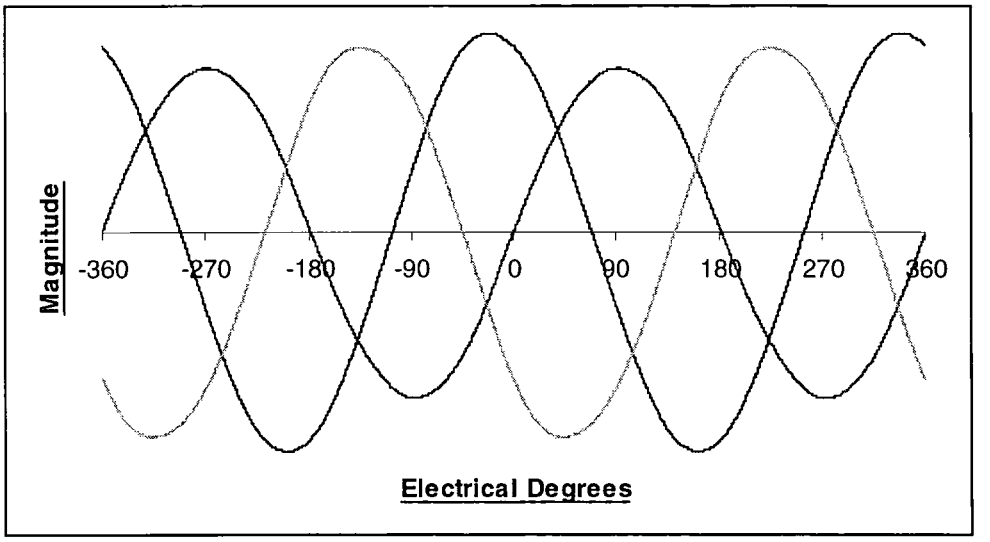

Fig. 7.11: BMVHM 3 phase emf distribution

From the open and short circuit results and Eqn. 6.4, a synchronous inductance of 8.8mH was calculated.

7.6.2 On Load Tests

On load tests were performed by connecting the generator output to a variable 3 phase resistive load. The load on the generator was then varied and the machine maintained at a constant speed. The measured power is presented in Fig. 7.12.

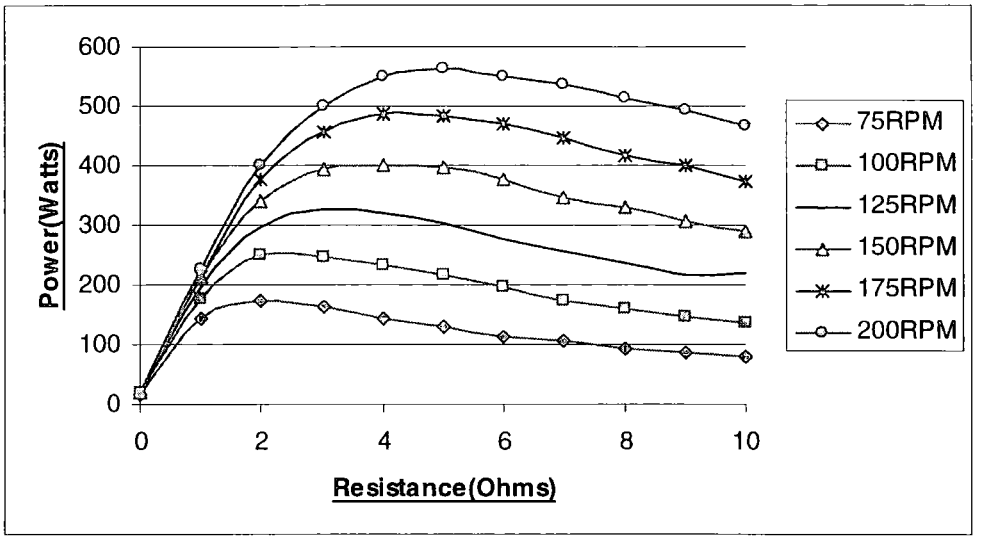

Fig. 7.12: On load output power characteristics

At the maximum speed of 200RPM, the peak power transferred is 565W which equates to a torque of 27Nm.

7.6.3 Capacitor Tests

As the VHM has a poor power factor, it is beneficial to provide some power factor correction. This is achieved by adding a bank of capacitors in parallel with the generator coils. The value of the capacitor bank required for adjusting the power factor to unity is calculated using Eqn. 7.4, for known values of the inductance and speed. In this case the capacitor bank values are large because the machine operates at such a low speed, for example, at 200RPM a value of 380μF per phase is needed.

$$C = \frac{1}{\omega^2 L} \qquad \text{Eqn. 7.4}$$

The value of the capacitor bank installed was 400μF per phase. At a resistive load of 10Ω per phase and speed of 130RPM, the output power is 502W (37Nm), which shows an increase of 128% above the power of 220W obtained without power factor correction

Fig. 7.13 shows the output power for a 10Ω load with and without power factor correction. By using the DC drive motor, speeds in excess of 130RPM could not be achieved as the drive motor would stall, thus the resonance point was never reached.

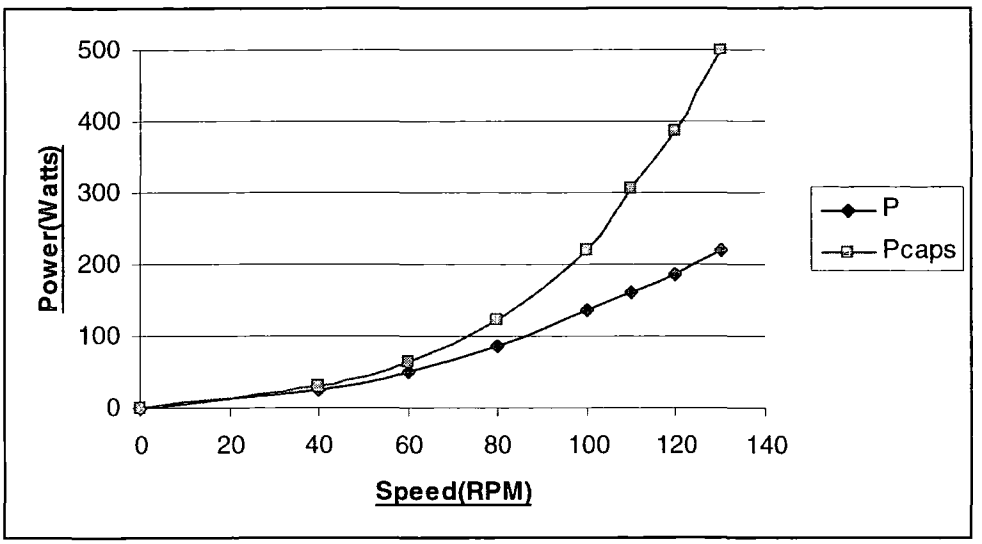

Fig. 7.13: Output power with and without capacative correction

7.7 Results Comparison

For the AFVHM the test results are not very close to the FEA predictions, partly because the input parameters to the FEA model are not so clearly defined. The airgap is especially hard to quantify as it varies with rotor position on both sides of the machine. Due to the construction method, the sum of both airgaps cannot be greater than 4mm. Fig. 7.14 depicts the measured results compared to 2D FEA (including 3D leakage calculated with Eqn. 6.6) with various airgap values.

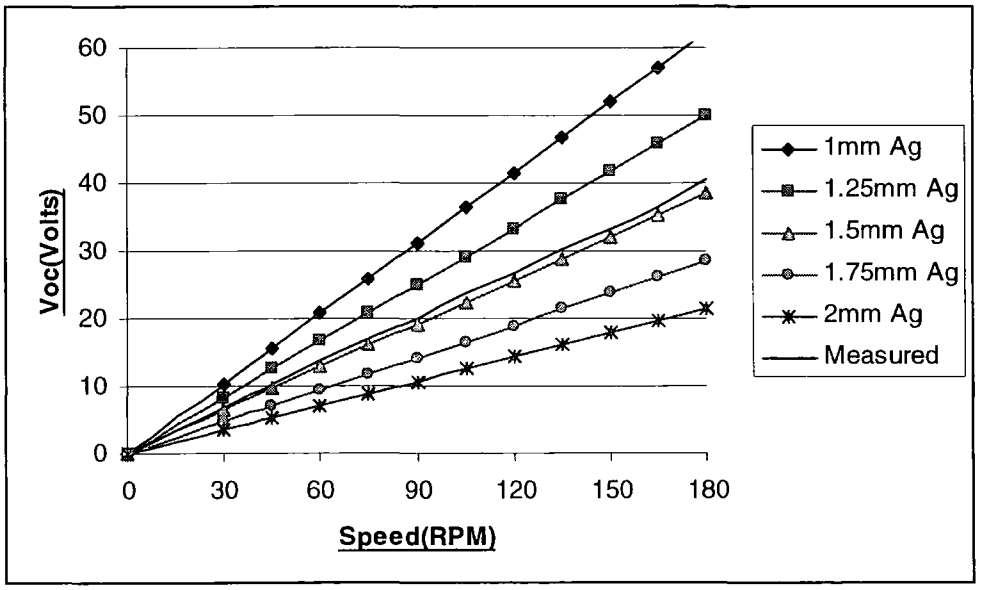

Fig. 7.14: FEA and measured results comparison for V_{oc} with varying airgap

The LP results use the same parameters as the FEA model and about the measured values the results are surprisingly close to the FEA, as shown in Fig. 7.15.

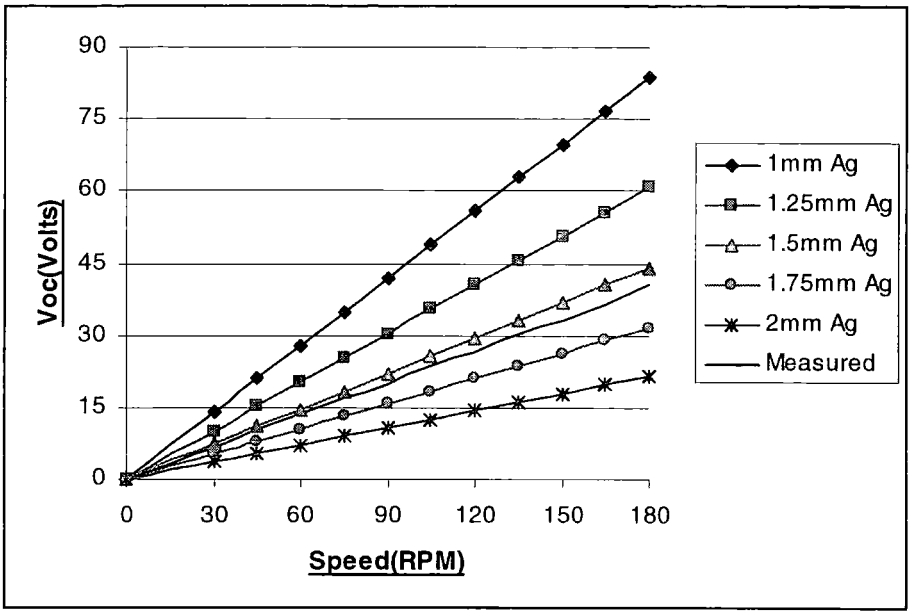

Fig. 7.15: FEA and LP results comparison for V_{oc} with varying airgap

8.0 Discussion and Further Work

8.1 Discussion

The VHM displays large shear stress and high power density values for greatly reduced rotor angular velocity. By a combination of these attributes the VHM lends itself to applications where slow high power rotational inputs are desired. As mentioned an application that perfectly matches these characteristics is wind turbine generation. The main reason for this suitability is that the gearbox can be omitted and direct drive applied.

In general the VHM exhibits the following characteristics:

- Robust rotor construction due to lack of magnets and coils makes for an easy to construct and balanced rotor. (this feature would also make the machine suited to a number of high speed applications).
- Uncomplicated stator pole geometry provides for simple and efficient concentric windings.
- Permanent magnet excitation, absence of excitation losses and no need for current transfer by brushes results in reduced maintenance requirements and makes remote applications more practicable.
- Permanent magnet material increases construction difficulty when compared to typical machines.
- Iron and magnet eddy current losses can be substantial due to the high frequency flux variations even for low rotational speeds.
- Low power factor is a major drawback as this adds increased expense with respect to correction and higher rated power electronics.

The BMVHM and AFVHM topologies both have differing advantages and disadvantages that are in addition to the general VHM. For the BMVHM:

- Increased flux linkages and magnetic loading are achievable through flux concentration.

- Construction is simplified by the radial flux nature and lack of permanent magnets in the airgap.

- Repelling magnets are easily mounted within the stator casing.

AFVHM has the following properties:

- Reduced eddy current losses in the magnets and surrounding material, which protects the magnets and minimises losses.

- Increased flux linkages and magnetic loading are achievable through flux concentration.

- Improved magnet utilisation and hence improved shear stress by the use of unidirectional mmfs across the magnets.

- Construction is difficult due to unusual design necessitated by 3D flux paths.

- Adjacent magnets repel which means that bonding must be used to keep the magnets attached to the steel.

- Support for the stator decreases coil winding area and introduces complexity with respect to insulation for eddy current reduction.

The previously mentioned characteristics qualify the VHM for some useful applications for both the motoring and generating form of operation. Most applications where a low rotational speed at high torque is required are suited to the VHM. Many unconsidered applications must exist but some of the considered applications include:

- Ship propulsion motors.

- Wind, tidal and wave energy converters.

- The linear form of the machine would be useful as a direct drive lift motor. This is of great interest for tall buildings because conventional lifts are limited by the weight of their cables.

- High speed gas turbine generators could use the VHM, exploiting the simple steel rotor's mechanical integrity. The electrical frequency would be very high and special design measures would be required.

8.2 Further Work

This study has explored buried magnet versions of the VHM topology and enabled a new variation to be designed and built. Further work should include more in depth study into the fundamental mechanisms of operation and would most likely start with comprehensive 3D analysis. More extensive testing on the AFVHM should also be conducted so that the maximum power values of the machine can be determined. This will require a connection to the Ward Leonard test rig so that the high driving torques can be achieved.

It is a concern that the properties of the permanent magnet material may vary from those specified and a study to the accuracy of these magnetic properties performed so that precise models may be defined. There is also the application of different materials to be considered. As the construction of the AFVHM is complicated it would be useful to use permeable materials with a degree of workability e.g., putty like compounds with good magnetic properties like those used for tool repair. There is also the option of utilising powdered ferrite as this can be moulded to almost any shape. The magnetic effects and limitations of these materials would need to be studied.

An economic viability study of both the AFVHM and BMVHM with respect to construction and performance over a rated lifetime specific to a chosen application is recommended along with a review of the construction procedures.

Study related to the power electronics needed to achieve direct drive variable speed generation and power factor correction is necessary. It may be found that each topology will benefit from different power electronic configurations. For the variable-speed mode of operation it may be beneficial to design a machine with more than 3 phases as the resulting rectified voltage will be smoother. More phases will also reduce the power ratings of individual power electronic modules that are used.

9.0 Conclusion

The VHM has high torque handling capabilities at low speeds, which enables the VHM to be built compactly and without gearing which suits wind power generation applications. It is also useful for high speed applications due to its robust rotor construction but increased iron losses are inevitable. Unfortunately, the VHM operates to the detriment of power factor and construction complexity.

Two prototype VHM's were developed and tested, a BMVHM and an AFVHM. The BMVHM exhibited all the positive attributes of the VHM with the added benefits of flux concentration and simple magnet embedding within the stator. The AFVHM also displayed the positive attributes with the addition of minimised losses in the magnets, better magnet utilisation and potentially higher torque rating. However, the construction and design of the AFVHM is substantial and is a major viability consideration.

10.0 Appendices

Appendix A: Typical N30 Properties

Some material properties and characteristics of the N30 type sintered rare earth NdFeB permanent magnet used for both prototypes.

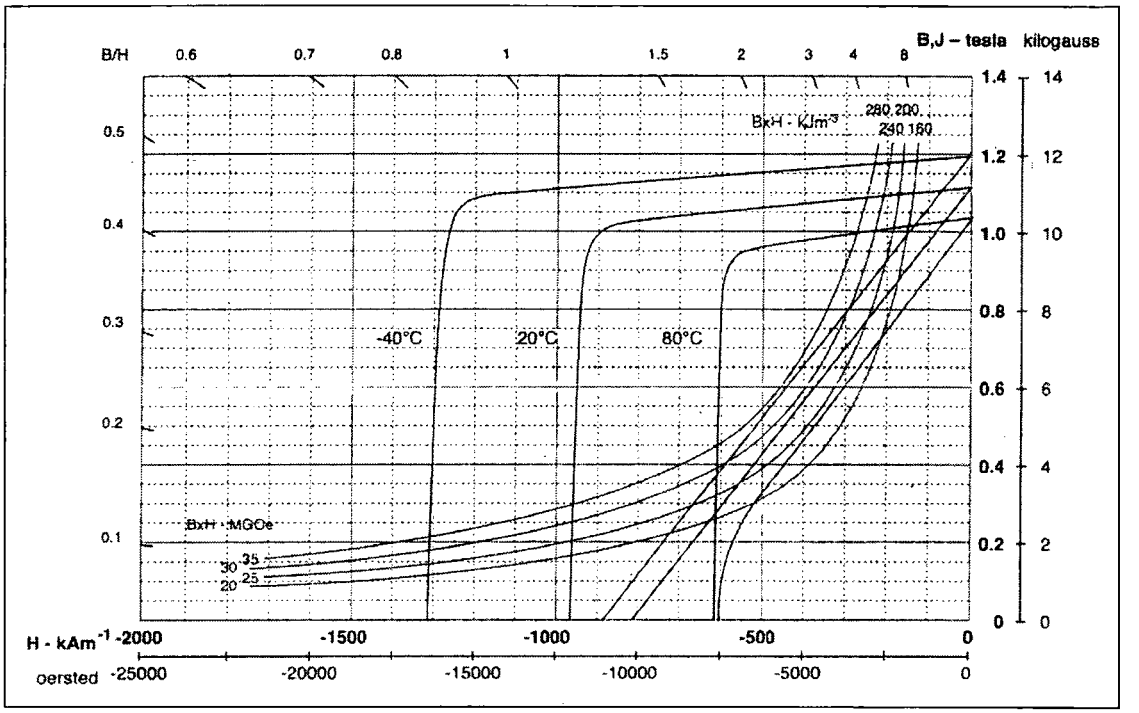

Fig. A.1: BH curves for N30 at varying temperatures.

Property	Value and unit
Remnance	1.12 T
Coercivity	835 kA/m
Maximum Energy Product	240 kJ/m^3
Temp coefficient of B_r	-0.12 %/°C
Density	7.4 g/cm^3
Relative Recoil Permeability	1.05
Curie Temperature	310°C
Continuous Maximum Operating Temp	80°C

Table A.1: Typical properties of N30 NdFeB

Appendix B: Electrical Magnetic Equivalents

Magnet:

A permanent magnet can be modelled like a battery, as a voltage source in series with a resistance. The voltage source is equivalent to the magnet mmf and the resistance is equivalent to the reluctance of the magnet. To quantify these values various dimensions and properties are required.

The magnet mmf is related to B_r of the magnet, the magnet thickness in the polarised direction (Fig. B.1) and the recoil permeability and permeability of free space by Eqn. B.1.

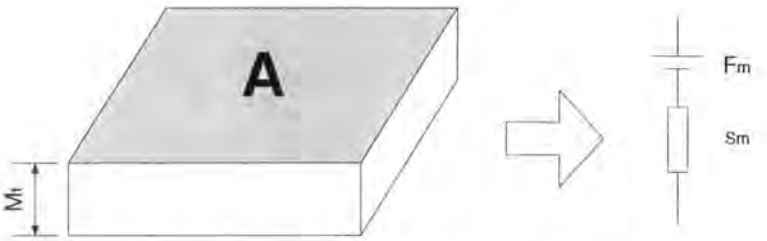

Fig. B.1: Electrical equivalent of a magnet

$$F_m = \frac{B_r M_t}{\mu_{rec}\mu_0} \qquad \text{Eqn. B.1}$$

The reluctance provided by the magnet is comparable to the major magnet dimensions and the recoil permeability and permeability of free space by Eqn. B.2.

$$S_m = \frac{M_t}{\mu_{rec}\mu_0 A} \qquad \text{Eqn. B.2}$$

Path Reluctance:

Reluctance of the airgap or any other material is modelled as equivalent to resistance by Eqn. B.3.

$$S_x = \frac{t_x}{\mu_{rx} A_x} \qquad \text{Eqn. B.3}$$

Where t_x is the path thickness i.e., the distance the flux must flow, A_x is the area of the path and μ_{rx} is the permeability of the material.

Appendix C: End Leakage Calculations

To derive the amount of end flux leakage a simplification of Amperes Law is required:

$$F = Hl = NI \qquad \text{Eqn. C.1}$$

When considering a magnet, N=1 and l=length of the arc,

$$H = \frac{I}{l} = \frac{I}{\pi r} \qquad \text{Eqn. C.2}$$

To get H in terms of flux we use flux density,

$$B = \mu H \qquad \text{Eqn. C.3}$$

By substitution,

$$B = \frac{\mu I}{\pi r} \qquad \text{Eqn. C.4}$$

As flux is related to flux density by area, integration between the two radii will provide a value for the leakage flux, where l is the length in the 3rd dimension, in this case magnet length, M_l,

$$\phi_l = \int_{r_1}^{r_2} Bldr = \frac{l\mu I}{\pi}\int\frac{1}{r}dr = \frac{M_l\mu I}{\pi}\left[\ln(r_2) - \ln(r_1)\right] \qquad \text{Eqn. C.5}$$

Appendix D: FEA Inductance Calculations

Self Inductance (L_{self}):

The self inductance is defined by the flux that links a coil that is induced by the current flowing in that coil by Eqn. D.1.

$$L_{self} = \frac{\psi}{I_{in}} \qquad \text{Eqn. D.1}$$

Where ψ is flux linkage and represented by,

$$\psi = N\phi \qquad \text{Eqn. D.2}$$

Mutual Inductance (Lm):

Mutual inductance is defined by the flux linking other coils in a magnetic circuit that is established by current in a reference coil by Eqn. D.3.

$$Lm_{a-b} = \frac{\psi_b}{I_a} \qquad \text{Eqn. D.3}$$

Where a is the reference coil and b is the measured coil. The total mutual inductance is the sum of the mutual inductances of all the coils in the circuit.

Leakage Inductance (L_l):

Leakage inductance is defined as the inductance attributed to the leakage flux paths. To calculate this in FEA the rotor is replaced with air so that the primary magnetic path no longer exists. The leakage inductance is then defined in the same manner as the self inductance.

Appendix E: AFVHM LP Equivalent Circuit

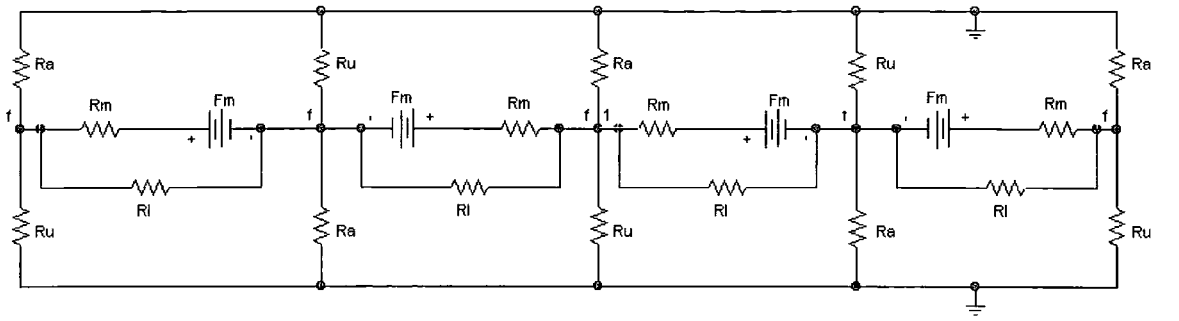

Fig. E.1: The equivalent electrical circuit for the AFVHM.

Eqn. B.1 is derived from Kirchoff's current law for node 1. Where F_{ml} and S_{ml} are the values after Thevinin and Norton equivalents have been used on the magnet mmf, F_m, leakage, S_l, and source reluctances, S_m. f is the potential of node 1.

$$\frac{f}{S_a}+\frac{f}{S_u}=\frac{F_{ml}-2f}{S_{ml}}+\frac{F_{ml}-2f}{S_{ml}} \qquad \text{Eqn. E.1}$$

Solving for f,

$$f=\left[\frac{2F}{4+\frac{S_{ml}}{S_a}+\frac{S_{ml}}{S_u}}\right] \qquad \text{Eqn. E.2}$$

f is the airgap mmf. The rotor back iron, on either side can be considered as a zero potential reference. From the airgap mmf and reluctance values, the flux for the aligned and misaligned rotor position is defined as:

$$\phi_a=\frac{f}{S_a} \qquad \text{Eqn. E.3}$$

$$\phi_u=\frac{f}{S_u} \qquad \text{Eqn. E.4}$$

Therefore the total flux for one unit in the aligned position equates to:

$$\phi=\phi_a-\phi_u \qquad \text{Eqn. E.5}$$

To calculate the coil inductance, the flux linkage due to coil current acting alone is needed. This results in the equivalent circuit of Fig. E.2, where the mmf of the magnet is omitted.

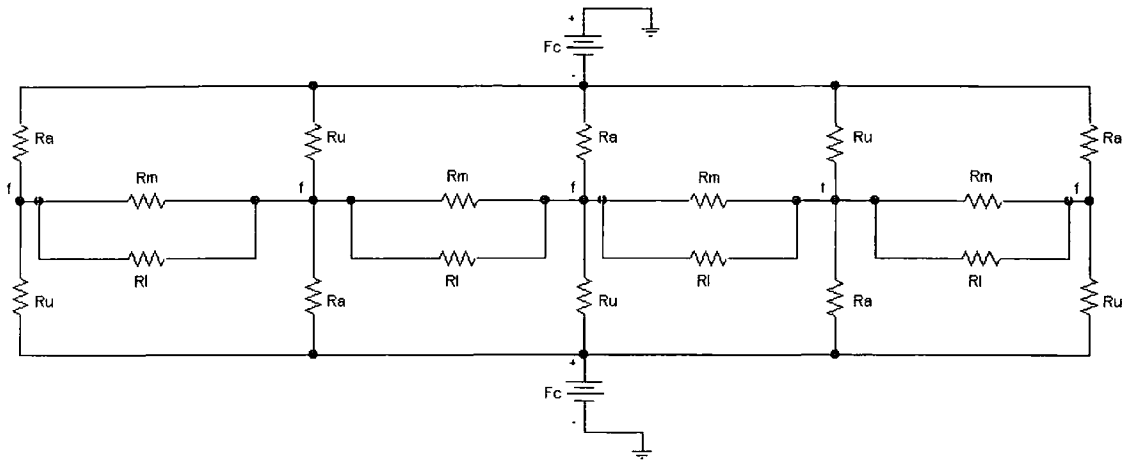

Fig. E.2: The equivalent electrical circuit for the AFVHM including the coil mmfs.

Kirchoff's current law defines Eqn. E.6.

$$\frac{f - F_c}{S_a} = \frac{-f - f}{S_{ml}} + \frac{-f - f}{S_{ml}} + \frac{-F_c - f}{S_u} \qquad \text{Eqn. E.6}$$

Solving for f,

$$\therefore f = \frac{F_c\left[\frac{1}{S_a} + \frac{1}{S_u}\right]}{\left[\frac{4}{S_{ml}} + \frac{1}{S_a} + \frac{1}{S_u}\right]} \qquad \text{Eqn. E.7}$$

To determine the aligned (Φ_{ac}) and unaligned flux (Φ_{uc}) the coil mmf must now also be included.

$$\phi_{ac} = \frac{F_c - f}{S_a} \qquad \text{Eqn. E.8}$$

$$\phi_{uc} = \frac{F_c + f}{S_u} \qquad \text{Eqn. E.9}$$

Using the values of flux for the aligned and unaligned positions, with and without coil excitation, the short circuit mmf of the coil can be found, Eqn. E.10.

$$F_{sc} = \frac{\phi_a - \phi_u}{\phi_{ac} - \phi_{uc}} \qquad \text{Eqn. E.10}$$

For a speed of 1m/s, the frequency can be solved.

$$f = \frac{1}{P_p} \qquad \text{Eqn. E.11}$$

Hence the RMS emf can also be calculated using the flux from Eqn. E.5.

$$e = \frac{\omega\phi}{\sqrt{2}} \qquad \text{Eqn. E.12}$$

For a purely resistive load, the maximum power transfer occurs when the load resistance equals the internal machine resistance.

$$V @ P\max = \frac{e}{\sqrt{2}} \qquad \text{Eqn. E.13}$$

$$I @ P\max = \frac{F_{sc}}{\sqrt{2}} \qquad \text{Eqn. E.14}$$

$$P = VI \qquad \text{Eqn. E.15}$$

Appendix F: Turn Number Calculations

To determine the number of turns per coil the rated speed and output voltage of the machine is required. In this case the rated speed is chosen at approximately 300RPM and the output voltage must be less than $400V_{dc}$ when rectified.

By using the FEA results for flux linkage with 3D losses accounted for, the generated emf at 300RPM can be calculated from Faradays Law.

$$e = N\frac{d\phi}{dt} = N\frac{d\phi}{d\theta} * \frac{d\theta}{dt} = N\omega\frac{d\phi}{d\theta} \qquad \text{Eqn. F.1}$$

For the VHM the flux linkage has a sinusoidal distribution which enables the peak flux linkage and emf to be easily determined.

$$\hat{e} = N\omega\hat{\phi} \qquad \text{Eqn. F.2}$$

This emf is peak and in terms of line to neutral voltage so to calculate the total output from a 3 phase diode bridge rectifier,

$$V_{dc} = \frac{3\sqrt{3}}{\pi}e \qquad \text{Eqn. F.3}$$

Therefore, for values of N=160, RPM=300, $\hat{\phi} = 0.0011Wb$ the output voltage of the rectifier is, 235V which is well below the 400V limit and will decrease more so as the machine is loaded.

Appendix G: Photographs

BMVHM:

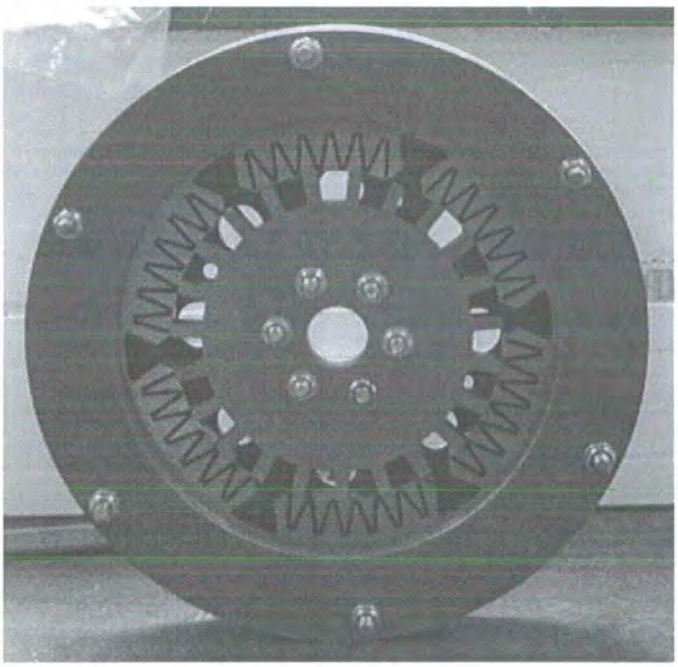

Fig. G.1: BMVHM with no coils or magnets inserted

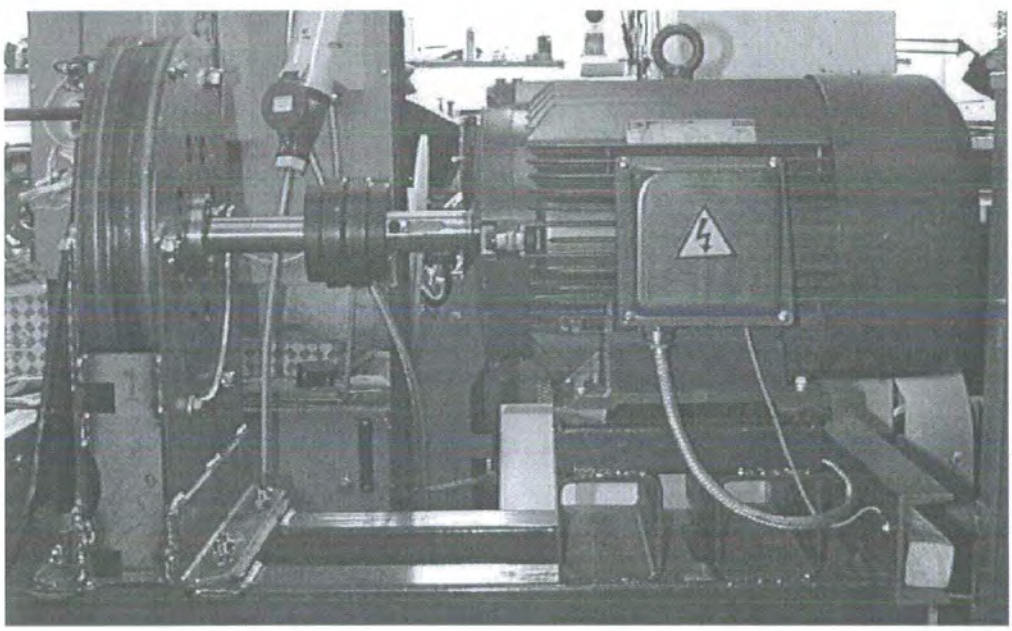

Fig. G.2: The BMVHM test rig

AFVHM:

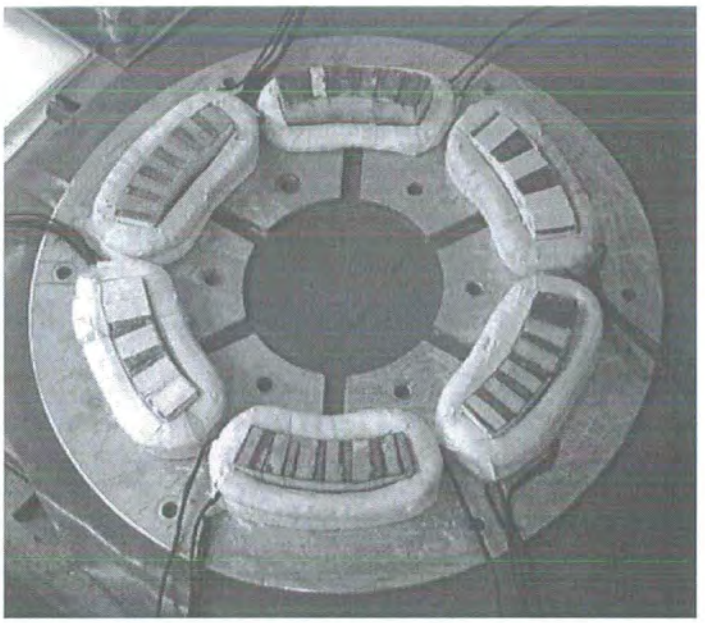

Fig. G.3: AFVHM stator showing coils, stator blocks and 1 aluminium support

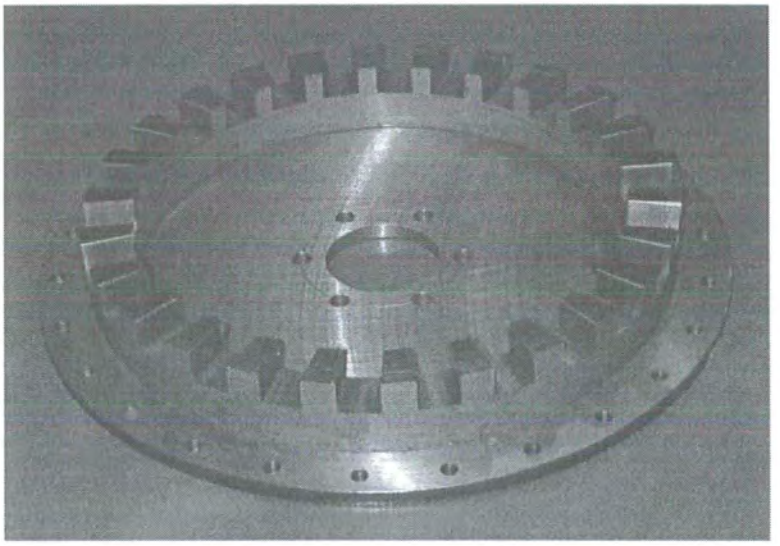

Fig. G.4: One rotor side of the AFVHM

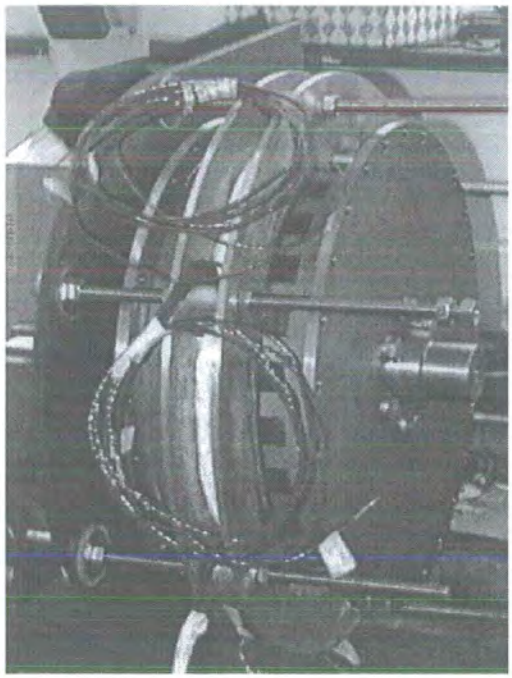

Fig. G.5: Assembly of the AFVHM

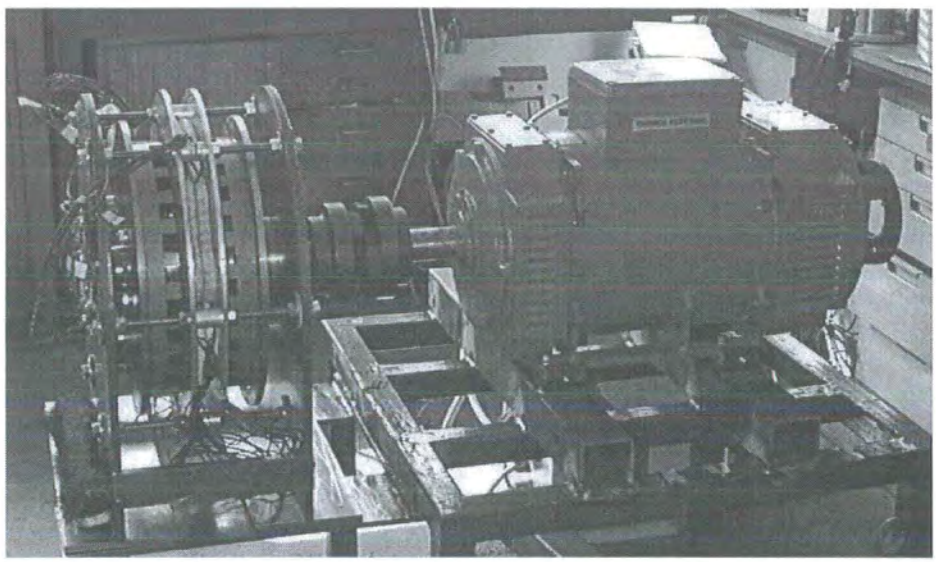

Fig. G.6: AFVHM test rig

11.0 References

1) Weh, H., Hoffmann, H., Landrath, J.: "New Permanent Magnet Excited Synchronous Machine with High Efficiency at Low speeds", ICEM, Pisa Italy, 1988, pp 35-40

2) Mecrow, B.C., Jack, A.G.: "A New High Torque Density Permanent Magnet Machine Configuration", Proc. International Conference of Electrical Machines, Cambridge USA, 1990, pp1046-1052 (Vol 3)

3) Deodar, R.P., Andersson, S., Boldea, I., Miller, T.J.E.: "The Flux-Reversal Machine: A New Brushless Doubly Salient Permanent-Magnet Machine", IEEE Trans. of Industry Applications, 1997, pp 925-933 (Vol 33, No 4)

4) Spooner, E., Haydock, L.: "Vernier Hybrid Machines", submitted to IEE Proc. Electrical Power Applications.

5) Miller, T.J.E.: "Brushless Permanent Magnet and Reluctance Motor Drives", Clarendon Press, 1989

6) Amin, B.: "High-Density Torque Motor Structures", ICEM, Espoo Finland, 2000, pp1936-1940 (Vol1)

7) Roding, W.E.: "Wind Energy by Rim Generation Using Brushless DC Technology", Undergraduate Project Report, Auckland University, 1999

8) Boyle, G.: "Renewable Energy: Power for a Sustainable Future", Oxford University Press, 1996, pp267-314

9) Keppola, H. et al: "Preliminary Test Results of an Axial Flux Toroidal Stator Wind Power Generator", ICEM, Espoo Finland, 2000, pp1480-1484 (Vol 3)

10) Chen, Z.: "Advanced Wind Energy Converters Using Electronic Power Conversion", PhD, 1997, pp20-22

11) Spooner, E., Mueller, M.A.: "Experimental Design of Electromechanical Devices", to be submitted to IEE Proceedings part B.

12) Roding, W.E., Spooner, E.: "The Design of Axial-Airgap Transverse-Flux Machines", UPEC, Swansea UK, 2001

13) Brown, N., Haydock, L., Spooner, E., Bumby, J.: "Optimisation of Axial Flux Generators by Pre-Computed 3D-FEA Modelling", ICEM, Espoo Finland, 2000, pp1471-1474 (Vol 1)

14) Edwards, J.D.: "Electrical Machines: An Introduction to Principles and Charecteristics", Intertext books, 1973, pp 24-27

15) Lampola, P., Saransaari, P.: "Analysis of a Multipole, Low speed Permanent-Magnet Synchronous Machine", ICEM, Espoo Finland, 2000, pp1251-1255 (Vol 3)

16) Llibre, J.F., Matt, D.: "Vernier Reluctance Magnet Machine for Electric Vehicle", ICEM, 1994, pp 251-256 (Vol 1)

17) Harris, M.R., Pajooman, G.H., Abu Sharkh, S.M.: "The Problem of Power Factor in VRPM (Transverse-Flux) Machines", IEE Proc. Electrical Machines and Drives, Cambridge UK, 1997, pp386-390

18) Salo, J., Heikkilä, T., Pyrhönen, J., Haring, T.: "New Low speed High-Torque Permanent Magnet Machine with Buried Magnets", ICEM, Espoo Finland, 2000, pp1246-1250 (Vol 3)

19) Schaefer, J.: "Rectifier Circuits: Theory and Design", John Wiley and Sons Inc., 1965

20) Smith, A.C.: "Magnetic Forces on a Misaligned Rotor of a PM Linear Actuator", ICEM, 1990, pp1076-1081 (Vol3)